RSC Advances

PAPER

View Article Online
View Journal | View Issue

Cite this: *RSC Adv.*, 2018, **8**, 7315

Syntheses, crystal structures, magnetic properties and ESI-MS studies of a series of trinuclear $Cu^{II}M^{II}Cu^{II}$ compounds (M = Cu, Ni, Co, Fe, Mn, Zn)†

Nairita Hari,[a] Shuvankar Mandal,[a] Arpita Jana,[a] Hazel A. Sparkes[b] and Sasankasekhar Mohanta *[a]

Six trinuclear $Cu^{II}M^{II}Cu^{II}$ compounds (M = Cu, Ni, Co, Fe, Mn, Zn) derived from the Schiff base ligand, H_2L (2 + 1 condensation product of salicylaldehyde and *trans*-1,2-diaminocyclohexane) are reported in this investigation. The composition of the metal complexes are $[\{Cu^{II}L(ClO_4)\}_2Cu^{II}(H_2O)]\cdot 2H_2O$ (**1**), $[\{Cu^{II}L(ClO_4)\}\{Ni^{II}(H_2O)_2\}\{Cu^{II}L\}]ClO_4\cdot CH_3COCH_3$ (**2**), $[\{Cu^{II}L(ClO_4)\}\{Co^{II}(CH_3COCH_3)(H_2O)\}\{Cu^{II}L(CH_3COCH_3)\}]ClO_4$ (**3**) and isomorphic $[\{Cu^{II}L(ClO_4)\}_2M^{II}(CH_3OH)_2]$ (**4**, M = Fe; **5**, M = Mn; **6**, M = Zn). Two copper(II) ions in **1–6** occupy N_2O_2 compartments of two L^{2-} ligands, while the second metal ion occupies the $O(phenoxo)_4$ site provided by the two ligands, *i.e.*, the two metal ions in both $Cu^{II}M^{II}$ pairs are diphenoxo-bridged. Positive ESI-MS of **1–6** reveals some interesting features. Variable-temperature and variable-field magnetic studies reveal moderate or weak antiferromagnetic interactions in **1–6** with the following values of magnetic exchange integrals ($H = -2JS_1S_2$ type): $J_1 = -136.50$ cm^{-1} and $J = 0.00$ for the $Cu^{II}Cu^{II}Cu^{II}$ compound **1**; $J_1 = -22.16$ cm^{-1} and $J = -1.97$ cm^{-1} for the $Cu^{II}Ni^{II}Cu^{II}$ compound **2**; $J_1 = -14.78$ cm^{-1} and $J = -1.86$ cm^{-1} for the $Cu^{II}Co^{II}Cu^{II}$ compound **3**; $J_1 = -6.35$ cm^{-1} and $J = -1.17$ cm^{-1} for the $Cu^{II}Fe^{II}Cu^{II}$ compound **4**; $J_1 = -6.02$ cm^{-1} and $J = -1.70$ cm^{-1} for the $Cu^{II}Mn^{II}Cu^{II}$ compound **5**; $J = -2.25$ cm^{-1} for the $Cu^{II}Zn^{II}Cu^{II}$ compound **6** (J is between two Cu^{II} in the N_2O_2 compartments; J_1 is between Cu^{II} and M^{II} through a diphenoxo bridge).

Received 30th December 2017
Accepted 5th February 2018

DOI: 10.1039/c7ra13763j

rsc.li/rsc-advances

Introduction

A major goal in the research of magnetochemistry is the establishment of magneto-structural correlations[1] so that magnetic properties of new compounds can be predicted and the intimate relationship of spin coupling can be better rationalized. Although the magnetic exchange interaction in discrete molecules was reported for the first time in the early 1950s,[2] the first straightforward magneto-structural correlation was reported in 1976 when Hatfield, Hodgson and coworkers established a linear correlation between the magnetic exchange integral and the Cu–O–Cu hydroxo bridge angle in planar dihydroxo-bridged dicopper(II) compounds.[3] Later, a number of experimental and theoretical correlations have been determined in varieties of systems. Most of the concerned systems are homometallic such as bis(μ-hydroxo)/bis(μ-alkoxo)/bis(μ-phenoxo)/bis(μ-halide)/bis($\mu_{1,1}$-azide)/bis($\mu_{1,3}$-azide)/μ-phenoxo dicopper(II) compounds,[4] linear tricopper(II) compounds where the two metal ions in a copper(II)···copper(II) pair are diphenoxo-bridged,[5] alkoxo-bridged tetracopper(II) systems,[6] bis(μ-phenoxo)/bis($\mu_{1,1}$-azide)/bis($\mu_{1,3}$-azide)/bis(μ-oximato)/μ-phenoxo-$\mu_{1,1}$-azide dinickel(II) compounds,[4e–g,7] end-to-end azide bridged tetranickel(II) compounds,[8] μ-oxo/bis(μ-dialkoxo) diiron(III) compounds,[9a,b] hexairon(III) systems having μ-hydroxo-bis(μ-carboxylate)/bis(μ-alkoxo)-μ-carboxylate bridging moiety between two metal ions,[9c] bis($\mu_{1,1}$-azide) dimanganese(II) compounds,[4d] bis(μ-oxo) dimanganese(IV) compounds,[9d] tris(μ-hydroxo)/tris(μ-oxo)tris(μ-ethoxide)/tris(μ-chloride)/tris(μ-bromide)/tris(μ-iodide)/μ-oxo-bis(μ-hydroxo)/bis(μ-oxo)-μ-hydroxo dimanganese(IV)/divanadium(II)/dichromium(III) compounds,[9e] radical bridged digadolinium(III) systems,[10] *etc.* In comparison to those in homometallic systems, the correlations in heterometallic systems are only a few and those are the experimental correlations in diphenoxo-bridged copper(II)···gadolinium(III)[11a]/copper(II)···oxovanadium(IV)[11b]/iron(III)···nickel(II)[11c] compounds and theoretical correlations in diphenoxo-bridged copper(II)···gadolinium(III)[11d]/nickel(II)···gadolinium(III)[11e]/iron(III)···nickel(II)[11f] systems. Hence, syntheses, and magnetic studies of new heterometallic systems deserves attention so that magneto-structural correlations in heterometallic systems may be established.

The Schiff base ligands obtained on the [2 + 1] condensation of salicylaldehyde/2-hydroxyacetophenone/2-hydroxypropiophenone/

[a]*Department of Chemistry, University of Calcutta, 92 A. P. C. Road, Kolkata 700 009, India. E-mail: sm_cu_chem@yahoo.co.in; Fax: +91-33-23519755*

[b]*School of Chemistry, University of Bristol, Cantock's Close, Bristol, BS8 1TS, UK*

† Electronic supplementary information (ESI) available: Structural, magnetic and ESI-MS schemes, figures and tables (Scheme S1, Fig. S1–S27, Tables S1–S8). CCDC 1584530–1584535 for **1–6**, respectively. For ESI and crystallographic data in CIF or other electronic format see DOI: 10.1039/c7ra13763j

3-methoxysalicylaldehyde/3-ethoxysalicylaldehyde and a diamine (such as ethylenediamine, 1,3-diaminopropane, *trans*-1,2-diaminocyclohexane, *o*-phenylenediamine, 2,2-dimethyl-1,3-diaminopropane, *etc.*) belong to an excellent class of ligands to stabilize homo/heterometallic systems,[12–24] most of which, in turn, are important in the research areas of exchange-coupled systems. The synthesis procedure involves the isolation of a 3d mononuclear metallo-ligand (such as a Cu^{II} metallo-ligand) in which the metal ion occupies the $N(imine)_2O(phenoxo)_2$ compartment. The treatment of the metallo-ligand with a second metal ion produces homo/heterometallic systems. The reason of the incorporation of two metal ions per ligand is the bridging ability of the phenoxo oxygen atoms and, from that perspective, all the above mentioned ligands may be considered as similar. It is also worth mentioning that a copper(II) metallo-ligand has been mostly utilized to derive homo/heterometallic systems following metallo-ligand + second metal ion approach. Although a lot of compounds have been reported from the above mentioned ligands, exploration of the metal complexes from a new or a less utilized ligand always deserves attention due to the possibility of getting new aspects in terms of structures and properties. To be noted that the particular Schiff base ligand (H_2L; Scheme 1) containing salicylaldehyde as the aldehyde counterpart and *trans*-1,2-diaminocyclohexane as the diamine counterpart has only been rarely utilized to derive copper(II)–second metal ion compounds,[12,24] although many copper(II)–second metal ion systems are known from closely similar ligands.[12–23] Therefore, we thought to explore the copper(II)–second metal ion complexes from this ligand as a part of our continuous contribution to enrich the homo/heterometallic systems from the above mentioned types of ligands.[11c,13i,14h,i,15a,b,19i–m,20a,22,23] Accordingly, we have reacted $[Cu^{II}L]$ with the perchlorate salts of copper(II), nickel(II), cobalt(II), iron(II), manganese(II) and zinc(II) and isolated six trinuclear $Cu^{II}M^{II}Cu^{II}$ compounds. Herein, we report the syntheses, crystal structures, variable-temperature and variable-field magnetic properties and electrospray ionization mass spectra in positive mode (ESI-MS positive) of the derived six compounds.

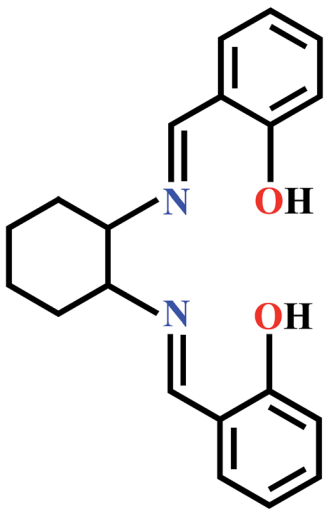

Scheme 1 Chemical structure of H_2L.

Experimental section

Caution! Perchlorate complexes of metal ions with organic ligands are potentially explosive. Only a small amount of material should be prepared, and it should be handled with care.

Materials and physical measurements

All the reagents and solvents were purchased from commercial sources and used as received. $[Cu^{II}L]$ was synthesized by a known procedure.[24] Elemental (C, H and N) analyses were performed on a Perkin-Elmer 2400 II analyzer. IR spectra were recorded in the region 400–4000 cm^{-1} on a Bruker-Optics Alpha-T spectrophotometer with samples as KBr disks. The electrospray ionization mass spectra were recorded on a Waters Xevo G2 QTOF Mass Spectrometer. Magnetic data were collected with a SQUID-VSM (Quantum Design) instrument.

Syntheses

$[\{Cu^{II}L(ClO_4)\}_2Cu^{II}(H_2O)]\cdot 2H_2O$ (1), $[\{Cu^{II}L(ClO_4)\}\{Ni^{II}(H_2O)_2\}\{Cu^{II}L\}]ClO_4\cdot CH_3COCH_3$ (2) and $[\{Cu^{II}L(ClO_4)\}\{Co^{II}(CH_3COCH_3)(H_2O)\}\{Cu^{II}L(CH_3COCH_3)\}]ClO_4$ (3). These three compounds were prepared following a general procedure, as follows: an acetone solution (2 mL) of the corresponding $M(ClO_4)_2\cdot 6H_2O$ (0.15 mmol; M = Cu/Ni/Co) was dropwise added to a stirred suspension of $[Cu^{II}L]$ (0.115 g, 0.3 mmol) in acetone (3 mL). The mixture was stirred for 30 minutes. The bright red/wine red solution was filtered into a long tube and to the filtrate diethyl ether was added very slowly to make two separate layers. Then, the tube was stoppered and kept undisturbed. After a few days, a red crystalline compound was formed which was collected by filtration, washed with cold acetone and dried in vacuum. Recrystallization from acetone-diethylether in a long tube produced red crystalline compound containing diffractable single crystals.

*Data for **1**.* Yield: 0.130 g (80%). Anal. calc. for $C_{40}H_{46}N_4O_{15}Cl_2Cu_3$: C, 44.31; H, 4.28; N, 5.17. Found: C, 44.72; H, 4.09; N, 5.35. FT-IR (cm^{-1}, KBr): [$\nu(H_2O)$] 3441m; [ν(C=N)] 1638vs; [$\nu(ClO_4^-)$] 1099vs, 620s.

*Data for **2**.* Yield: 0.125 g (75%). Anal. calc. for $C_{43}H_{50}N_4O_{15}Cl_2Cu_2Ni$: C, 46.13; H, 4.50; N, 5.00. Found: C, 45.78; H, 4.39; N, 4.82. FT-IR (cm^{-1}, KBr): [$\nu(H_2O)$] 3418m; [ν(C=N)] 1637vs; [$\nu(ClO_4^-)$] 1095vs, 626s.

*Data for **3**.* Yield: 0.140 g (80%). Anal. calc. for $C_{46}H_{54}N_4O_{15}Cl_2Cu_2Co$: C, 47.63; H, 4.69; N, 4.83. Found: C, 47.94; H, 4.78; N, 5.05. FT-IR (cm^{-1}, KBr): [$\nu(H_2O)$] 3420m; [ν(C=N)] 1636vs; [$\nu(ClO_4^-)$] 1094vs, 625s.

$[\{Cu^{II}L(ClO_4)\}_2Fe^{II}(CH_3OH)_2]$ (4) and $[\{Cu^{II}L(ClO_4)\}_2Mn^{II}(CH_3OH)_2]$ (5). These two compounds were prepared following the similar procedure as that for **1–3**. The only difference is that, here methanol was used instead of acetone and $M(ClO_4)_2\cdot xH_2O$ (M = Fe/Mn) was used instead of $M(ClO_4)_2\cdot 6H_2O$ (M = Cu/Ni/Co).

*Data for **4**.* Yield: 0.105 g (65%). Anal. calc. for $C_{42}H_{48}N_4O_{14}Cl_2Cu_2Fe$: C, 46.42; H, 4.45; N, 5.16. Found: C, 46.26; H, 4.28; N,

5.30. FT-IR (cm^{-1}, KBr): [ν(C=N)] 1636vs; [$\nu(ClO_4^-)$] 1095vs, 623s.

Data for ***5****.* Yield: 0.098 g (60%). Anal. calc. for $C_{42}H_{48}N_4O_{14}Cl_2Cu_2Mn$: C, 46.46; H, 4.46; N, 5.16. Found: C, 46.29; H, 4.40; N, 5.25. FT-IR (cm^{-1}, KBr): [ν(C=N)] 1636vs; [$\nu(ClO_4^-)$] 1107vs, 624s.

[{$Cu^{II}L(ClO_4)$}$_2Zn^{II}(CH_3OH)_2$] (6). A methanol solution (5 mL) of $Zn(ClO_4)_2\cdot 6H_2O$ (0.15 mmol) was dropwise added to a stirred suspension of [Cu^{II}L] (0.1152 g, 0.3 mmol) in methanol (10 mL). The mixture was stirred for 30 minutes. The resulting violet solution was filtered and the filtrate was kept at room temperature for slow evaporation. After a few days, red crystalline compound containing diffractable single crystals that deposited was collected by filtration, washed with cold methanol, and dried in vacuum. Yield: 0.115 g (70%). Anal. calc. for $C_{42}H_{48}N_4O_{14}Cl_2Cu_2Zn$: C, 46.02; H, 4.41; N, 5.11. Found: C, 46.31; H, 4.34; N, 5.28. FT-IR (cm^{-1}, KBr): [ν(C=N)] 1637vs; [$\nu(ClO_4^-)$] 1093vs, 623s.

Crystal structure determination of 1–6

The crystallographic data for **1–6** are summarized in Table 1. X-ray diffraction data were collected on a Bruker-APEX II SMART CCD diffractometer at 296(2) K using graphite-monochromated Mo Kα radiation (λ = 0.71073 Å). For data processing, the SAINT packages were used.[25a] All data were corrected for Lorentz-polarization effects. Multiscan absorption correction were made for all the six cases using the program SADABS.[25b] Structures were solved by direct and Fourier methods and refined by full-matrix least-squares based on F^2 using SHELXL.[25c,d] All of the non-hydrogen atoms were refined anisotropically. While all of the hydrogen atoms were located geometrically and refined using a riding model with the exception of the water hydrogen atoms in **1** and **3** which were located in the difference map and refined with the O–H distance restrained. In the case of **3**, the structure was refined as a racemic twin, giving a twin scale fraction of 0.20(2). In addition Squeeze within Platon[25e,f] was used to remove disordered solvent that could not be sensibly modelled from the lattices of **1** and **2**. The electron counts per unit cell for the eliminated solvent molecules are 42 and 124 (31 per void) for **1** and **2**, respectively, indicating the presence of two water molecules (Z = 2 in **1**) and one acetone molecule (Z = 4 in **2**) as solvent of crystallization in the molecular formula. In **2**, **3**, **4**, **5** and **6** the perchlorate ions were disordered over two positions, the occupancies of the two orientations were refined with their sum set to equal 1. Restraints and constraints were applied to maintain sensible thermal and geometric parameters for the disordered atoms. In addition to the perchlorate disorder, **2**, **4**, **5** and **6** also showed full or partial disorder in the cyclohexane ring, the occupancies of the atoms were refined with their sum set to equal 1, restraints and constraints were also applied to maintain sensible thermal and geometric parameters for the disordered atoms.

The final refinement converged at the R_1 ($I > 2\sigma(I)$) values of 0.0687, 0.0448, 0.0395, 0.0427, 0.0368 and 0.0943 for **1–6**, respectively.

Results and discussion

Syntheses and characterization of 1–6

The trinuclear $Cu^{II}M^{II}Cu^{II}$ compounds **1–6** were readily prepared in good yield on treating [Cu^{II}L] with $M(ClO_4)_2\cdot 6H_2O$/$M(ClO_4)_2\cdot xH_2O$ in 2 : 1 stoichiometric ratio in acetone-diethylether for **1** (M = Cu), **2** (M = Ni) and **3** (M = Co), in methanol-diethylether for **4** (M = Fe) and **5** (M = Mn) and in methanol for **6** (M = Zn). Reaction of [Cu^{II}L] and $M(ClO_4)_2\cdot 6H_2O$ in 1 : 1 ratio also produced the compounds **1–6** but the yield is reduced, revealing that trinuclear $Cu^{II}M^{II}Cu^{II}$ systems are more stable in this ligand ($[L]^{2-}$) environment in comparison to systems of other nuclearity. It is also worth mentioning that solvent has a profound role in the isolation of these compounds, *e.g.*, **1–3** and **4** and **5** could not isolated in crystalline form on evaporating the concerned reaction mixture in acetone and methanol, respectively, while crystalline compounds are isolated on diffusing the reaction solution with diethylether. It is also worth mentioning that **1–3** could not be isolated in methanol-diethylether and **4** and **5** could not be isolated from acetone-diethylether. Only the zinc(II) analogue **6** could be isolated in crystalline form on slow evaporation of the reaction solution (in methanol). Inspite of the variation required in solvent and technique (diffusion/evaporation), all the six compounds **1–6** are trinuclear in which a pair of $Cu^{II}M^{II}$ metal ions are solely diphenoxo bridged. We would like to mention that isolation of the five compounds **1–5** in crystalline form was troublesome, which may be a reason that the copper(II)–second metal ion compounds derived from H_2L is just two till date,[24] while such compounds from closely related ligands are too many. It may be mentioned that although several salicylaldehyde/2-hydroxyacetophenone/2-hydroxypropiophenone/3-methoxysalicylaldehyde/3-ethoxysalicylaldehyde–diamine ligands were previously utilized to derive copper(II)–second metal ion compounds, compounds with all the six second metal ions from Mn^{II} to Zn^{II} are rare; to the best of our knowledge, copper(II)–zinc(II)/copper(II)/nickel(II)/cobalt(II)/iron(II)/manganese(II) systems were reported from one ligand, 3-ethoxysalicylaldehyde–ethylenediamine,[23a–d] although the composition of all those six compounds are not similar – cocrystals of one dinuclear $Cu^{II}M^{II}$ and two mononuclear Cu^{II} units when M = Zn/Cu/Co/Fe/Mn but either a trinuclear $Cu^{II}Ni^{II}Cu^{II}$ or a cocrystal of one trinuclear $Cu^{II}Ni^{II}Cu^{II}$ and two mononuclear Cu^{II} moieties when M = Ni. Hence, H_2L herein is the second ligand of the above mentioned general class of Schiff base ligands where it has been possible to isolate/report all the six copper(II)–zinc(II)/copper(II)/nickel(II)/cobalt(II)/iron(II)/manganese(II) systems and, all the six are similar in composition, trinuclear $Cu^{II}M^{II}Cu^{II}$ systems.

The characteristic C=N stretching in **1–6** appears as a strong band at practically the same position, 1636–1638 cm^{-1}. The appearance of one signal of strong intensity in the range 1093–1107 cm^{-1} and a medium intensity in the range 620–626 cm^{-1} indicates the presence of perchlorate. Compounds **1–3** exhibit a band of medium intensity in the range 3418–3441 cm^{-1}, indicative of the presence of water molecules.

Table 1 Crystallographic data for **1–6**

	$Cu^{II}Cu^{II}Cu^{II}$ (**1**)	$Cu^{II}Ni^{II}Cu^{II}$ (**2**)	$Cu^{II}Co^{II}Cu^{II}$ (**3**)	$Cu^{II}Fe^{II}Cu^{II}$ (**4**)	$Cu^{II}Mn^{II}Cu^{II}$ (**5**)	$Cu^{II}Zn^{II}Cu^{II}$ (**6**)
Empirical formula	$C_{40}H_{42}N_4O_{13}Cl_2Cu_3$	$C_{40}H_{44}N_4O_{14}Cl_2Cu_2Ni$	$C_{46}H_{54}N_4O_{15}Cl_2Cu_2Co$	$C_{42}H_{48}N_4O_{14}Cl_2Cu_2Fe$	$C_{42}H_{48}N_4O_{14}Cl_2Cu_2Mn$	$C_{42}H_{48}N_4O_{14}Cl_2Cu_2Zn$
Formula weight	1048.29	1061.48	1159.84	1086.67	1085.76	1096.19
Crystal color	Red	Red	Red	Red	Red	Red
Crystal system	Triclinic	Monoclinic	Monoclinic	Monoclinic	Monoclinic	Monoclinic
Space group	$P\bar{1}$	$P2_1/n$	Cc	$C2/c$	$C2/c$	$C2/c$
a/Å	10.021(2)	10.9788(6)	20.9449(9)	16.0994(12)	16.287(9)	16.200(19)
b/Å	13.993(3)	23.9304(13)	13.2515(6)	12.1164(9)	12.113(6)	12.254(15)
c/Å	15.997(4)	18.3403(10)	19.8004(9)	24.2086(18)	24.283(13)	24.32(3)
α/°	89.031(8)	90.00	90.00	90.00	90.00	90.00
β/°	80.648(8)	91.497(2)	112.976(2)	107.775(2)	108.528(7)	108.149(15)
γ/°	80.267(8)	90.00	90.00	90.00	90.00	90.00
V/Å^3	2181.3(8)	4816.8(5)	5059.6(4)	4496.9(6)	4542(4)	4589(9)
Z	2	4	4	4	4	4
T/K	296(2)	296(2)	296(2)	296(2)	296(2)	296(2)
2θ range for data collection/°	2.58–50.052	2.798–51.348	3.73–51.43	3.534–51.388	4.274–51.1	4.248–50.046
μ/mm^{-1}	1.640	1.437	1.332	1.446	1.390	1.623
ρ_{calcd}/g cm^{-3}	1.596	1.464	1.523	1.605	1.588	1.587
F(000)	1070	2176	2388	2232	2228	2248
Crystal size/mm^3	0.1 × 0.09 × 0.08	0.12 × 0.11 × 0.08	0.8 × 0.12 × 0.1	0.14 × 0.12 × 0.09	0.12 × 0.11 × 0.08	0.8 × 0.12 × 0.1
Radiation	MoKα ($\lambda = 0.71073$)	MoKα ($\lambda = 0.71073$)	MoKα ($\lambda = 0.71073$)	MoKα ($\lambda = 0.71073$)	MoKα ($\lambda = 0.71073$)	MoKα ($\lambda = 0.71073$)
Absorption correction	Multi-scan	Multi-scan	Multi-scan	Multi-scan	Multi-scan	Multi-scan
Index ranges	$-11 \le h \le 10$	$-13 \le h \le 13$	$-25 \le h \le 25$	$-16 \le h \le 19$	$-19 \le h \le 19$	$-19 \le h \le 19$
	$-16 \le k \le 16$	$-29 \le k \le 27$	$-16 \le k \le 15$	$-14 \le k \le 14$	$-14 \le k \le 12$	$-14 \le k \le 14$
	$-19 \le l \le 19$	$-22 \le l \le 22$	$-24 \le l \le 23$	$-29 \le l \le 29$	$-28 \le l \le 29$	$-28 \le l \le 28$
Reflections collected	25662	57816	34320	24823	16140	13690
Independent reflections	7658	9103	9017	4256	4230	4018
R_{int}, R_{sigma}	0.1060, 0.1171	0.0665, 0.0454	0.0278, 0.0291	0.0377, 0.0285	0.0348, 0.0351	0.1132, 0.1302
Data/restraints/parameters	7658/12/559	9103/608/711	9017/259/643	4256/84/309	4230/318/354	4018/318/354
Goodness-of-fit on F^2	0.979	1.027	1.040	1.087	1.040	0.977
$R_1{}^a$, $wR_2{}^b$ [$I > 2\sigma(I)$]	0.0687, 0.1607	0.0448, 0.1116	0.0395, 0.1053	0.0427, 0.1108	0.0368, 0.0925	0.0943, 0.2252
$R_1{}^a$, $wR_2{}^b$ (for all data)	0.1435, 0.2022	0.0781, 0.1291	0.0440, 0.1091	0.0529, 0.1187	0.0504, 0.1006	0.1387, 0.2693
Largest diff. peak/hole/e Å^{-3}	0.78/−0.90	0.65/−0.32	0.57/−1.12	0.77/−0.46	0.51/−0.33	1.48/−2.04

^{a} $R_1 = [\sum||F_o| - |F_c||/\sum|F_o|]$. ^{b} $wR_2 = [\sum w(F_o{}^2 - F_c{}^2)^2/\sum wF_o{}^4]^{1/2}$.

Description of crystal structures of 1–6

The crystal structures of **1–6** are shown in Fig. 1–3, S13, S2 and S3,† respectively. The structures reveal that all the six compounds are trinuclear $Cu^{II}M^{II}Cu^{II}$ systems (M = Cu (**1**), Ni (**2**), Co (**3**), Fe (**4**), Mn (**5**), Zn (**6**)). In each structure, there are two L^{2-} ligands and the $N(imine)_2O(phenoxo)_2$ compartment of each L^{2-} is occupied by a copper(II) ion. The two $[Cu^{II}L]$ moieties in each structure are so disposed that a $O(phenoxo)_4$ site is generated and that site is occupied by a second metal ion (Cu (**1**), Ni (**2**), Co (**3**), Fe (**4**), Mn (**5**), Zn (**6**)). Clearly, the metal ion in the $O(phenoxo)_4$ site and each of the two copper(II) ions in the $N(imine)_2O(phenoxo)_2$ compartment are diphenoxo bridged. Except tetracoordinated Cu2 centre in the $Cu^{II}Ni^{II}Cu^{II}$ compound **2**, all other copper(II) centres in the $N(imine)_2$-$O(phenoxo)_2$ compartment are pentacoordinated; the fifth coordination position is occupied by a perchlorate oxygen atom for Cu1 and Cu2 in **1**, Cu1 in **2**, Cu1 in **3**, Cu1/Cu1D in **4**, **5** and **6**, and by the oxygen atom of an acetone molecule for Cu2 in **3**. Regarding the second metal ion (in the $O(phenoxo)_4$ site), copper(II) centre in **1** is pentacoordinated but other metal ions (Ni^{II}, Co^{II}, Fe^{II}, Mn^{II} and Zn^{II}) are hexacoordinated. The fifth or fifth and sixth coordination site (s) is/are occupied by the following: the oxygen atom of a water molecule for Cu3 in **1**; two oxygen atoms of two water molecules for Ni1 in **2**; the oxygen atom of a water molecule and the oxygen atom of an acetone molecule for Co1 in **3**; two oxygen atoms of two methanol molecules for Fe1/Mn1/Zn1 in **4**/**5**/**6**. There are two water molecules in **1** and one acetone molecule in **2** as solvent of

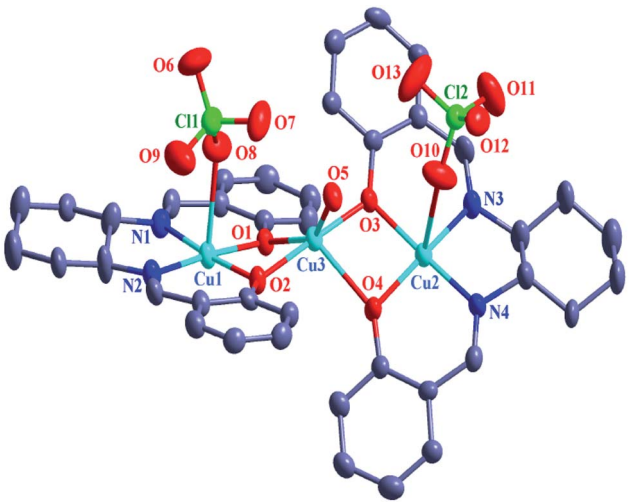

Fig. 1 ORTEP drawing (ellipsoid probability at 30%) of the structure of $[\{Cu^{II}L(ClO_4)\}_2Cu^{II}(H_2O)]\cdot 2H_2O$ (**1**). All hydrogen atoms are omitted for clarity.

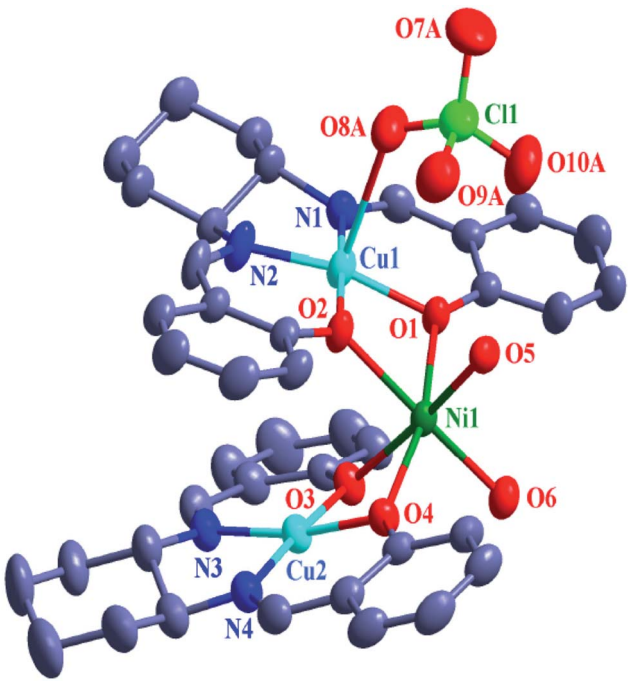

Fig. 2 ORTEP drawing (ellipsoid probability at 30%) of the structure of $[\{Cu^{II}L(ClO_4)\}\{Ni^{II}(H_2O)_2\}\{Cu^{II}L\}]ClO_4\cdot CH_3COCH_3$ (**2**). All hydrogen atoms and one perchlorate anion, are omitted for clarity.

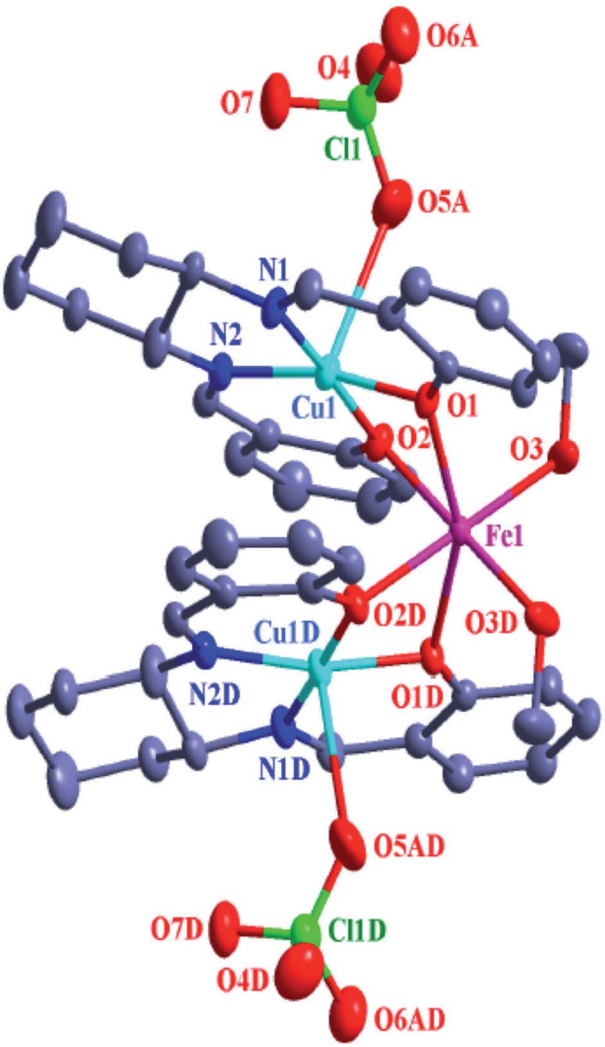

Fig. 3 ORTEP drawing (ellipsoid probability at 30%) of the structure of $[\{Cu^{II}L(ClO_4)\}_2Fe^{II}(CH_3OH)_2]$ (**4**). All hydrogen atoms are omitted for clarity. Symmetry code: *D*, 1 − *x*, *y*, 0.5 − *z*.

crystallization, while there is no solvent of crystallization in the other four structures. It is also worth mentioning that each of the compounds **4–6** crystallizes in monoclinic space group and *C*2/*c* crystal system with very close unit cell parameters (Table 1) and so these four compounds are isomorphous. One half of the structure of each of **4–6** is symmetry related to the second half.

The arrangement of the three metal ions in all of **1–6** is triangular; isosceles in **4–6** and closely isosceles in **1–3** (Scheme S1†). The Cu1···Cu3···Cu2, Cu1···Ni1···Cu2, Cu1···Co1···Cu2, Cu1···Fe1···Cu2, Cu1···Mn1···Cu2, and Cu1···Zn1···Cu2 angles in **1–6** are, respectively, 155.42°, 94.48°, 93.00°, 84.67°, 83.14° and 83.14°, while the other two metal···metal···metal angles in the triangular arrangement in **1–6** are, respectively, 12.53/12.05°, 42.48/43.03°, 43.63/43.37°, 47.67/47.67°, 48.43/48.43° and 48.43/48.43°. The distances of the two copper(II) centres in the $N(imine)_2O(phenoxo)_2$ compartments (*i.e.*, Cu1···Cu2) in **1–6** are, respectively, 5.802 Å, 4.365 Å, 4.383 Å, 4.105 Å, 4.102 Å and 4.047 Å, while the other two metal···metal distances in the triangular arrangement in **1–6** are, respectively, 2.919/3.027 Å, 2.988/2.957 Å, 3.014/3.028 Å, 3.048/3.048 Å, 3.091/3.091 Å and 3.050/3.050 Å.

The structural parameters around the copper(II) centres in the $N(imine)_2O(phenoxo)_2$ compartment in **1–6** are listed in Table S1.† The geometry of the coordination environment of the copper(II) centres in the $N(imine)_2O(phenoxo)_2$ compartment is distorted square planar for Cu2 in **2** and distorted square pyramidal ($N(imine)_2O(phenoxo)_2$ is the basal plane) for others in **1–6**; the value of the discrimination parameter, τ ($\alpha - \beta/60$, where α is the largest angle and β is the second largest angle in the coordination environment) for Cu1 and Cu2 in **1** are 0.005 and 0.012 and those for the copper(II) centres in **2–6** lie in the range 0.144–0.178. The Cu–O/N distances for the copper(II) centres in the $N(imine)_2O(phenoxo)_2$ compartment have close values; the overall ranges of the Cu–O and Cu–N distances in **1–6** are 1.895–1.928 Å and 1.889–1.935 Å, respectively. In comparison to the bond distances involving phenoxo/imine O/N atoms in the basal plane, the Cu–O(apical) distances involving an oxygen atom of perchlorate/acetone are significantly longer (the overall range in **1–6** is 2.596–2.868 Å), which is expected for copper(II) due to Jahn Teller distortion. The overall range of the transoid and cisoid angles in **1–6** are 166.4–178.6° and 81.3–105.51°, respectively. Notably, the values of the structural parameters around copper(II) in the $N(imine)_2O(phenoxo)_2$ compartment in **1–6** are in the ranges of those in the previously reported systems from related ligands.[13,16,17,19,23a–d,24]

The values of some structural parameters around the second metal ions (the metal ions in the $O(phenoxo)_4$ site) are compared in Tables 2 and 3. Of such metal centres, only copper(II) (Cu3) in **1** is pentacoordinated and the concerned τ value is 0.52, which indicates that this coordination environment is intermediate between square pyramidal and trigonal bipyramidal. The copper(II)–O(phenoxo) bond distances lie in the wide range of 1.937–2.214 Å, while the copper(II)–O(water) bond distance is 2.00 Å. The coordination environment of nickel(II), cobalt(II), iron(II), manganese(II) and zinc(II) in **2–6** is highly distorted octahedral as evidenced by the ranges of transoid and cisoid angles – the ranges of the transoid angles are 165.35–173.81° for Ni^{II}, 163.17–170.2° for Co^{II}, 153.40–175.86° for Fe^{II}, 150.24–174.56° for Mn^{II} and 152.0–176.4° for Zn^{II} and the ranges of the cisoid angles are 75.52–99.22° for Ni^{II}, 72.96–100.8° for Co^{II}, and 72.29–111.12° for Fe^{II} and 71.31–113.55° for Mn^{II} and 72.98–110.4° for Zn^{II}. In all of **2–6**, the M^{II}–O(water/methanol/acetone) bond distances are smaller than the M^{II}–O(phenoxo) bond distances – the average M^{II}–O(phenoxo) bond distances are 2.082 Å for Ni^{II}, 2.118 Å for Co^{II}, 2.152 Å for Fe^{II}, 2.201 Å for Mn^{II} and 2.149 Å for Zn^{II} and the average M^{II}–O(water/methanol/acetone) bond distances are 2.030 Å for Ni^{II}, 2.075 Å for Co^{II}, 2.078 Å for Fe^{II}, 2.153 Å for Mn^{II} and 2.073 Å for Zn^{II}.

The two Cu–O–Cu phenoxo bridge angles involving Cu1 and Cu3 are 95.9 and 98.0° and those involving Cu2 and Cu3 are

Table 2 Comparison of some structural parameters (distances in Å and angles in °) around the second metal ions in **1–6**

	1 (M = Cu^{II})	**2** (M = Ni^{II})	**3** (M = Co^{II})	**4** (M = Fe^{II})	**5** (M = Mn^{II})	**6** (M = Zn^{II})
Number and type of ligands	4 phenoxo, 1 water	4 phenoxo, 2 water	4 phenoxo, 1 water, 1 acetone	4 phenoxo, 2 methanol	4 phenoxo, 2 methanol	4 phenoxo, 2 methanol
Coordination number	5	6	6	6	6	6
M–O(phenoxo)	1.937, 1.947, 2.012, 2.214	2.060, 2.077, 2.087, 2.103	2.083, 2.123, 2.125, 2.141	2.134, 2.171	2.187, 2.215	2.129, 2.169
M–O(water)	2.000	2.024, 2.037	2.064	—	—	—
M–O(MeOH)	—	—	—	2.078	2.153	2.073
M–O(acetone)	—	—	2.086	—	—	—
Cu···M	2.9119 (with Cu1), 3.0266 (with Cu2)	2.9878 (with Cu1), 2.9573 (with Cu2)	3.0137 (with Cu1), 3.0282 (with Cu2)	3.0480 (with Cu1)	3.0908 (with Cu1)	3.050 (with Cu1)
Transoid angle range	145.268–176.5	165.35–173.81	163.17–170.2	153.40–175.86	150.24–174.56	152.0–176.4
Cisoid angle range	75.5–115.4	75.52–99.22	72.96–100.8	72.29–111.12	71.31–113.55	72.9–110.4
Discrimination parameter	0.5205	—	—	—	—	—
d_M	0.2929 (sq py), 0.0155 (tbp)	0.0049	0.0275	0.000	0.000	0.000
d_{av}	0.2821 (sq py), 0.000 (tbp)	0.1013	0.1384	0.0634	0.0927	0.0606

Table 3 Comparison of Cu–O(phenoxo)–M bridge angles, out-of-plane shifts and torsion angles (in °) in **1–6**

		1 (M = Cu^{II})	**2** (M = Ni^{II})	**3** (M = Co^{II})	**4** (M = Fe^{II})	**5** (M = Mn^{II})	**6** (M = Zn^{II})
Cu–O(phenoxo)–M bridge angles (α)	Cu1–O1–M	95.9	97.70	96.32	96.28	97.42	97.3
	Cu1–O2–M	98.0	96.16	98.00	97.74	96.73	96.2
	Cu2–O3–M	103.5	95.63	97.30	—	—	—
	Cu2–O4–M	94.5	95.79	96.35	—	—	—
Out of plane shift (φ)	O2–O1–C1	5.74	12.46	7.3	7.37	7.8	7.78
	O1–O2–C20	5.51	6.11	6.08	7.8	7.13	7.12
	O3–O4–C40	6.71	9.44	7.24	—	—	—
	O4–O3–C21	9.56	6.34	6.81	—	—	—
Torsion angle (τ)	Cu1–O1–M–O2	19.55	19.02	19.48	23.15	23.09	23.17
	Cu1–O2–M–O1	19.61	18.92	19.64	23.32	23.16	23.23
	Cu2–O3–M–O4	11.36	21.84	23.2	—	—	—
	Cu2–O4–M–O3	11.20	21.78	23.11	—	—	—

94.5° and 103.5°. In **2–6**, the four Cu–O–M phenoxo bridge angles not very different (95.63–97.70° in **2**, 96.32–98.00° in **3**, 96.28–97.74° in **4**, 96.73–97.42° in **5** and 96.2–97.3° in **6**); the average values are 96.32°, 96.99°, 97.01°, 97.07° and 96.75° for **2–6**, respectively.

Weak interactions in 1–6

There are three and two hydrogen bonds in, respectively, the $Cu^{II}Cu^{II}Cu^{II}$ compound **1** (Fig. S4†) and $Cu^{II}Ni^{II}Cu^{II}$ compound **2** (Fig. S5†). Of the three hydrogen bonds in **1**, two are O–H···O interactions (O5–H5A···O7, O5–H5B···O10) involving the coordinated water molecule and two oxygen atoms of two coordinated perchlorates. The remaining hydrogen bond in **1** is a C–H···O interaction involving a CH (C32H32B) hydrogen atom of a cyclohexane moiety and a perchlorate oxygen atom (O10E). The later interaction interlinks two trinuclear units to form a dimer-of-trinuclear type self-assembly. The two hydrogen bonds in **2** are O–H···O interactions (O5–H5B···O13E, O6–H6A···O11E) involving two coordinated water molecules and two oxygen atoms of one perchlorate anion. However, no supramolecular cluster or polymer is generated in **2**.

It was realized that the perchlorate oxygen atoms in **3** are engaged in few hydrogen bonding interactions. However, it is not possible to analyze the interactions or the supramolecular structure resulted therefrom due to disorder in most of the perchlorate oxygen atoms.

The OH (O3H3A) hydrogen atom of the crystallographically single type of coordinated methanol molecule in the $Cu^{II}Fe^{II}Cu^{II}$ compound **4** forms a hydrogen bond with one oxygen atom (O4E) of a perchlorate anion. One half of this compound is symmetry related to the second half in such a way that this O–H···O weak interaction generates a two-dimensional topology in the crystallographic *ab* plane (Fig. 4). The supramolecular topology of the $Cu^{II}Mn^{II}Cu^{II}$ compound **5** and

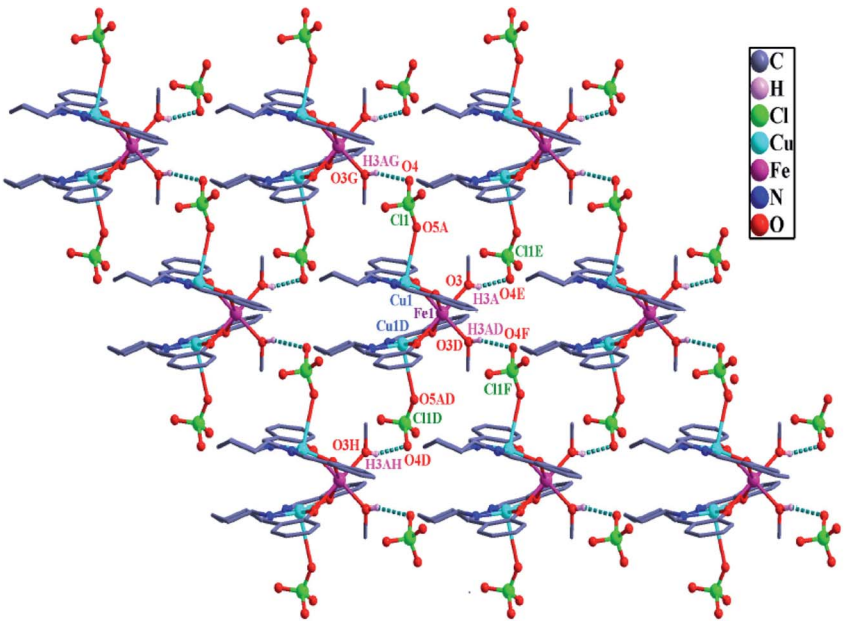

Fig. 4 Perspective view of the two-dimensional self-assembly in the crystallographic *ab* plane of $[\{Cu^{II}L(ClO_4)\}_2Fe^{II}(CH_3OH)_2]$ (**4**). Only the hydrogen atoms participating in hydrogen bonding interactions are shown. Symmetry: *D*, 1 − *x*, *y*, 0.5 − *z*; *E*, 0.5 − *x*, −0.5 + *y*, 0.5 − *z*; *F*, 0.5 + *x*, −0.5 + *y*, *z*; *G*, 0.5 − *x*, 0.5 + *y*, 0.5 − *z*; *H*, 0.5 + *x*, 0.5 + *y*, *z*.

$Cu^{II}Zn^{II}Cu^{II}$ compound **6**, which are isomorphous with **4**, are similar to that of **4** (corresponding illustrations for **5** and **6** are shown in Fig. S6 and S7,† respectively).

The values of the parameters of the hydrogen bonds in **1–6** are listed in Tables S2 and S3,† revealing that these interactions are moderately strong or weak.

ESI-MS positive studies of 1–6

ESI-MS of the methanol solution of **1** and acetonitrile solutions of **2–6** have been recorded. The observed and simulated spectra of the $Cu^{II}Ni^{II}Cu^{II}$ (**2**) and $Cu^{II}Mn^{II}Cu^{II}$ (**5**) compounds are shown in Fig. 5 and 6, respectively, while those of the $Cu^{II}Cu^{II}Cu^{II}$ (**1**), $Cu^{II}Co^{II}Cu^{II}$ (**3**), $Cu^{II}Fe^{II}Cu^{II}$ (**4**) and $Cu^{II}Zn^{II}Cu^{II}$ (**6**) compounds are shown in Fig. S8–S11,† respectively. The species appeared in the spectra are listed in Table 4 (without drawing) and Table S4† (with drawing). The line-to-line separation in a peak for the dipositive and monopositive ions are 0.5 and 1.0, respectively.

A total of fourteen types of species (**I–XIV**), which are tetra/tri/di/mononuclear, are observed in the spectra of the six compounds **1–6**, although no single type of ion corresponds to all the six compounds. The types of species involve a tetranuclear (possibly star) system of composition $[(Cu^{II}L)_3M^{II}]^{2+}$ (**I**), appeared in all the five heterometallic compounds **2–6**. Five types of trinuclear systems are appeared and those are: (i) $[(Cu^{II}L)M^{II}(ClO_4)(Cu^{II}L)]^+$ (**II**), which is the 100% intensity signal in all but the manganese(II) analogue; (ii) $[(Cu^{II}L)M^{I}(CH_3OH)(Cu^{II}L)]^+$ (**III**), which is the 100% intense peak in the manganese(II) analogue; (iii) $[(Cu^{II}L)M^{II}(Cu^{II}L)]^{2+}$ (**IV**), which appears in the five compounds **2–6**; (iv) $[(Cu^{II}L)M^{II}(ClO_4)(CH_3OH)(Cu^{II}L)]^+$ (**V**), which only appears in the iron(II) analogue; (v) $[(Cu^{II}L)(CH_3CN)M^{II}(ClO_4)(Cu^{II}L)(H_2O)]^+$ (**VI**), which appears only in the manganese(II) analogue. Four dinuclear ions that are observed are: (i) $[(Cu^{II}L)M^{II}(ClO_4)]^+$ (**VII**) which appears in the spectra of all but the iron(II) and manganese(II) analogues; (ii) $[(Cu^{II}L)M^{I}]^+$ (**VIII**) which appears in only the Cu^{II}_3 compound **1**; (iii) $[\{Cu^{II}(HL)\}(Cu^{II}L)]^+$ (**IX**) which appears in all but the manganese(II) analogue; (iv) $[\{Cu^{II}(HL)\}(Cu^{II}L)(CH_3COCH_3)]^+$ (**X**) which appears in **1** and **2** only. Four mononuclear ions are: (i) $[Cu^{II}(HL)]^+$ (**XI**; in **1**, **4** and **6**); (ii) $[Cu^{II}(H_2L)(ClO_4)]^+$ (**XII**; in all

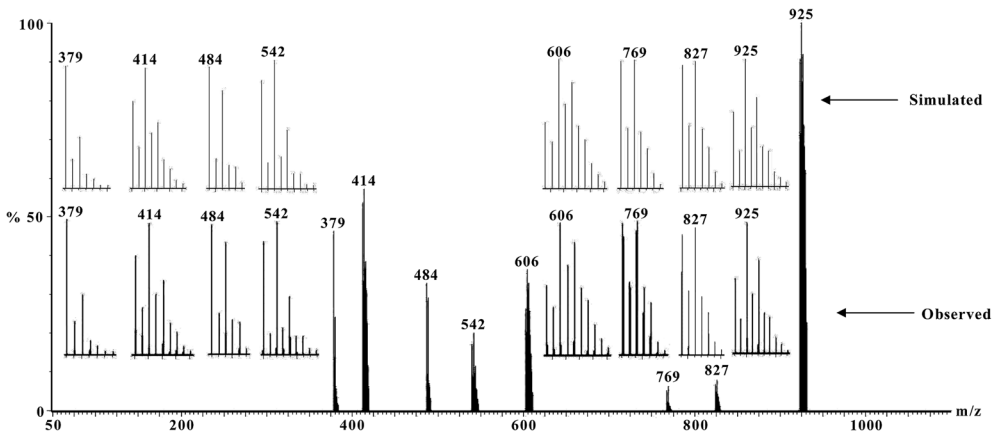

Fig. 5 Electrospray ionization mass spectrum in positive mode (ESI-MS positive) of $[\{Cu^{II}L(ClO_4)\}\{Ni^{II}(H_2O)_2\}\{Cu^{II}L\}]ClO_4\cdot CH_3COCH_3$ (**2**) in acetonitrile, showing observed and simulated isotopic distribution patterns.

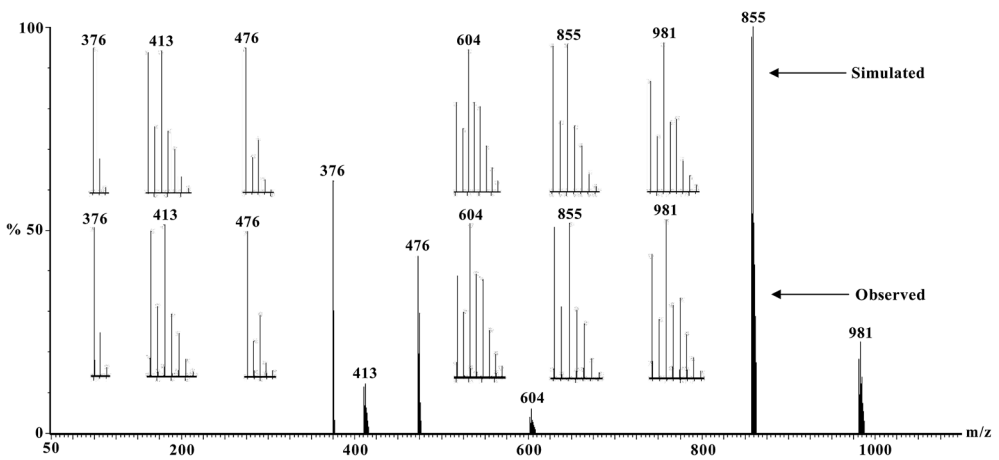

Fig. 6 Electrospray ionization mass spectrum in positive mode (ESI-MS positive) of $[\{Cu^{II}L(ClO_4)\}_2Mn^{II}(CH_3OH)_2]$ (**5**) in acetonitrile, showing observed and simulated isotopic distribution patterns.

Table 4 The composition, peak position and relative peak intensity of the species in the ESI-MS positive spectra of **1** in MeOH and **2–6** in MeCN

Ions in ESI-MS	Line-to-line *m/z* gap	**1** (M = Cu^{II}) Intensity	*m/z*	**2** (M = Ni^{II}) Intensity	*m/z*	**3** (M = Co^{II}) Intensity	*m/z*	**4** (M = Fe^{II}) Intensity	*m/z*	**5** (M = Mn^{II}) Intensity	*m/z*	**6** (M = Zn^{II}) Intensity	*m/z*
$[(Cu^{II}L)_3M^{II}]^{2+}$, (**I**; $C_{60}H_{60}N_6O_6Cu^{II}{}_3M^{II}$)	0.5	—	—	37%	606	12%	606	28%	605	6%	604	7%	610
$[(Cu^{II}L)M^{II}(ClO_4)(Cu^{II}L)]^+$, (**II**; $C_{40}H_{40}N_4O_8ClCu^{II}{}_2M^{II}$)	1.0	100%	930	100%	925	100%	926	100%	923	—	—	100%	931
$[(Cu^{II}L)M^{I}(CH_3OH)(Cu^{II}L)]^+$, (**III**; $C_{41}H_{44}N_4O_5Cu^{II}{}_2M^{I}$)	1.0	—	—	—	—	—	—	—	—	100%	855	—	—
$[(Cu^{II}L)M^{II}(Cu^{II}L)]^{2+}$, (**IV**; $C_{40}H_{40}N_4O_4Cu^{II}{}_2M^{II}$)	0.5	—	—	58%	414	59%	415	61%	412	12%	413	73%	417
$[(Cu^{II}L)M^{II}(ClO_4)(CH_3OH)(Cu^{II}L)]^+$, (**V**; $C_{41}H_{44}N_4O_9ClCu^{II}{}_2M^{II}$)	1.0	—	—	—	—	—	—	9%	955	—	—	—	—
$[(Cu^{II}L)(CH_3CN)M^{II}(ClO_4)(Cu^{II}L)(H_2O)]^+$, (**VI**; $C_{42}H_{45}N_5O_9ClCu^{II}{}_2M^{II}$)	1.0	—	—	—	—	—	—	—	—	23%	981	—	—
$[(Cu^{II}L)M^{II}(ClO_4)]^+$, (**VII**; $C_{20}H_{20}N_2O_6ClCu^{II}M^{II}$)	1.0	9%	547	21%	542	8%	542	—	—	—	—	24%	548
$[(Cu^{II}L)M^{I}]^+$, (**VIII**; $C_{20}H_{20}N_2O_2Cu^{II}M^{I}$)	1.0	9%	446	—	—	—	—	—	—	—	—	—	—
$[\{Cu^{II}(HL)\}(Cu^{II}L)]^+$, (**IX**; $C_{40}H_{41}N_4O_4Cu^{II}{}_2$)	1.0	12%	769	7%	769	5%	769	32%	769	—	—	7%	769
$[\{Cu^{II}(HL)\}(Cu^{II}L)(CH_3COCH_3)]^+$, (**X**; $C_{43}H_{47}N_4O_5Cu^{II}{}_2$)	1.0	83%	827	9%	827	—	—	—	—	—	—	—	—
$[Cu^{II}(HL)]^+$, (**XI**; $C_{20}H_{21}N_2O_2Cu^{II}$)	1.0	62%	384	—	—	—	—	43%	384	—	—	19%	384
$[Cu^{II}(H_2L)(ClO_4)]^+$, (**XII**; $C_{20}H_{22}N_2O_6ClCu^{II}$)	1.0	42%	484	33%	484	42%	484	60%	484	—	—	—	—
$[M^{II}(HL)]^+$, (**XIII**; $C_{20}H_{21}N_2O_2M^{II}$)	1.0	—	—	47%	379	46%	380	61%	377	63%	376	—	—
$[M^{II}(H_2L)(ClO_4)]^+$, (**XIV**; $C_{20}H_{22}N_2O_6ClM^{II}$)	1.0	—	—	—	—	—	—	—	—	44%	476	42%	485

but the manganese(II) and zinc(II) analogues); (iii) $[M^{II}(HL)]^+$ (**XIII**; in the four compounds **2–5**); (iv) $[M^{II}(H_2L)(ClO_4)]^+$ (**XIV**; in **5** and **6**).

Although the heteronuclear compounds **2–6** are trinuclear $Cu^{II}M^{II}Cu^{II}$ systems, ions of higher nuclearity, *i.e.*, the tetranuclear $[(Cu^{II}L)_3M^{II}]^{2+}$ (**I**) species, are stabilized in their ESI-MS. Most probably, such tetranuclear ions are star systems (Table S4†). It is worth mentioning that similar heterometallic star systems containing one Pb^{II} and three Cu^{II} (*i.e.*, $Pb^{II}Cu^{II}{}_3$) are also stabilized in the ESI-MS of trinuclear $Cu^{II}Pb^{II}Cu^{II}$ systems derived from closely similar single compartment ligands.[14i] Notably, star systems in solid state are rarely observed in the homo/heterometallic family derived from the ligands similar to H_2L.[15a,b,17f] From that perspective, the stabilization of star ions in the ESI-MS of all the five heterotrinuclear compounds **2–6** may be considered interesting. Another remarkable feature in the ESI-MS of **1–6** is the metal ion dependent stability of the 100% intense trinuclear ion. For the $Cu^{II}M^{II}Cu^{II}$ compounds **1–4** and **6** (M = Cu, Ni, Co, Fe and Zn), the 100% intense species is the trinuclear $Cu^{II}M^{II}Cu^{II}$ ion of composition $[(Cu^{II}L)M^{II}(ClO_4)(Cu^{II}L)]^+$ (**II**), which is not appeared in the spectrum of the Mn^{II} analogue **5**. On the other hand, the 100% intense ion in the spectrum of the $Cu^{II}Mn^{II}Cu^{II}$ compound **5** is a trinuclear $Cu^{II}Mn^{I}Cu^{II}$ species of composition $[(Cu^{II}L)Mn^{I}(CH_3OH)(Cu^{II}L)]^+$ (**III**) and such a species is not appeared in the spectra of the other five compounds **1–4** and **6**. This observation may be considered as interesting firstly due to the fact that **II** is the most intense ion in **1–4** and **6** and is not appeared in **5** while **III** is the most intense ion in **5** and is not appeared in **1–4** and **6** and secondly due to the fact that **III** is an unusual Mn^{I} species while **II** is an usual M^{II} (M = Cu, Ni, Co, Fe, Zn) species.

Magnetic properties of 1–6

Variable-temperature (2–300 K) $\chi_M T$ *versus* T plots for the $Cu^{II}M^{II}Cu^{II}$ compounds **1–6** are shown in Fig. 7 (for **1**; M = Cu), Fig. 8 (for **2**, **3**, **4** and **5**; M = Ni, Co, Fe, Mn) and Fig. S12† (for **6**; M = Zn). The $\chi_M T$ values (in $cm^3\ mol^{-1}\ K$) at 300 K for the $Cu^{II}Cu^{II}Cu^{II}$ (**1**), $Cu^{II}Ni^{II}Cu^{II}$ (**2**), $Cu^{II}Co^{II}Cu^{II}$ (**3**), $Cu^{II}Fe^{II}Cu^{II}$ (**4**), $Cu^{II}Mn^{II}Cu^{II}$ (**5**) and $Cu^{II}Zn^{II}Cu^{II}$ (**6**) compounds are, respectively, 0.78, 1.87, 3.23, 3.7, 4.96 and 0.89 while the spin-only theoretical values (with $g = 2.0$) of noninteracting metal ions (S = 1/2, 1, 3/2, 2 and 5/2 for Cu^{II}, Ni^{II}, Co^{II}, Fe^{II} and Mn^{II}, respectively) are, respectively, 1.12, 1.75, 2.62, 3.75, 5.12 and 0.75. So, while the observed and calculated values are not very different for the Ni^{II} (**2**), Fe^{II} (**4**), Mn^{II} (**5**) and Zn^{II} (**6**) analogues, the observed value is smaller by 0.34 and greater by 0.61 in the case of the Cu^{II} (**1**) and Co^{II} (**3**) analogues, respectively. On lowering of temperature, $\chi_M T$ values for all the six compounds **1–6** decrease throughout the temperature range. However, the pattern of decrease is different for the different compounds. For **1**, $\chi_M T$ values decrease sharply in the temperature range 300–100 K and then decrease slowly to 0.41 at 2 K. For the four compounds **2–5**, $\chi_M T$ values decrease slowly up to a certain temperature (*ca.* 100 K for **2** and **3** and *ca.* 80 K for **4** and **5**) and then decrease rapidly to the values of 0.001, 0.36, 0.43 and 1.82 at 2 K for **2–5**, respectively. For the Zn^{II} analogue **6**, $\chi_M T$

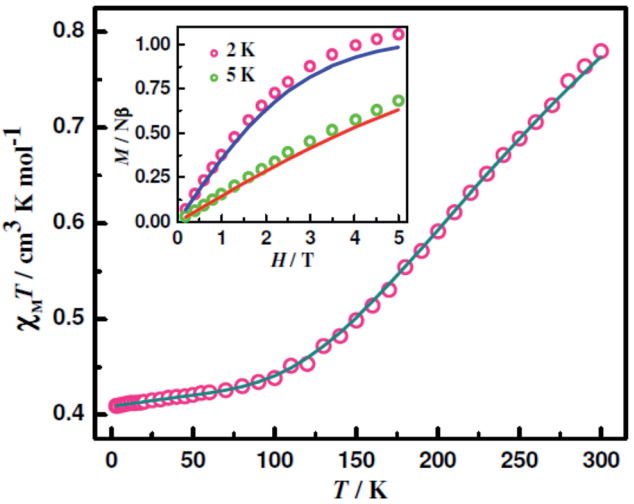

Fig. 7 Fitting of $\chi_M T$ *versus* T of $[\{Cu^{II}L(ClO_4)\}_2Cu^{II}(H_2O)]\cdot 2H_2O$ (**1**) between 2 and 300 K. The experimental data are shown in symbols and the lines correspond to the fitted values. The inset graph shows magnetization of $[\{Cu^{II}L(ClO_4)\}_2Cu^{II}(H_2O)]\cdot 2H_2O$ (**1**) at the indicated temperatures. The symbols are the experimental data, while the solid lines represent the fitted curves.

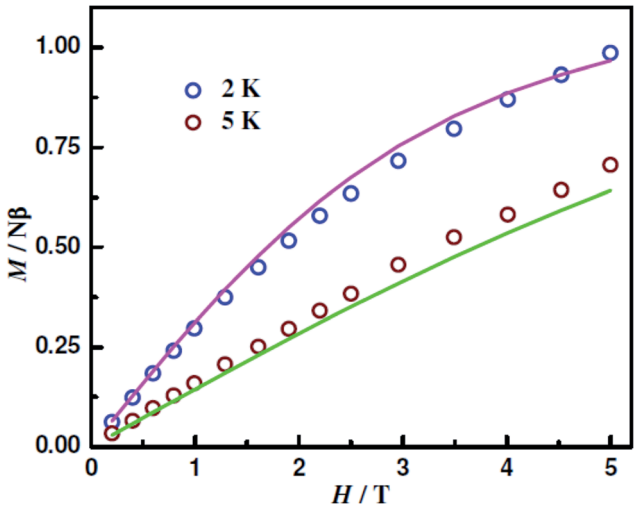

Fig. 9 Magnetization of $[\{Cu^{II}L(ClO_4)\}\{Co^{II}(CH_3COCH_3)(H_2O)\}\{Cu^{II}L(CH_3COCH_3)\}]ClO_4$ (**3**) at the indicated temperatures. The symbols are the experimental data, while the solid lines represent the fitted curves.

decreases very slowly in the temperature range 300–28 K (from 0.89 to 0.80) and then the values decrease sharply to 0.13 at 2 K. The profiles indicate that the metal centres are coupled by very weak antiferromagnetic interaction in **6**, by weak antiferromagnetic interaction in **2–5** and by moderate antiferromagnetic interaction in **1**.

The magnetization (M) data up to 5 T of **1–5** were collected at 2/2.5 and 5 K. For the Ni^{II} analogue (**2**), the M values even at 5 T are very small, less than 0.2, indicating its nonmagnetic ground state. The data of the other four compounds **1**, **3**, **4** and **5** are shown in Fig. 7, 9, 10 and S13,† respectively. The M values at 2 K and 5 T of 1.05 Nβ of the $Cu^{II}Cu^{II}Cu^{II}$ compound **1**, 0.99 Nβ of the $Cu^{II}Co^{II}Cu^{II}$ compound **3** and 3.06 Nβ of the $Cu^{II}Mn^{II}Cu^{II}$ compound **5** indicate that their spin ground states are, respectively, $S_T = 1/2$, $S_T = 1/2$ and $S_T = 3/2$. On the other hand, the M value at 2 K and 5 T of the $Cu^{II}Fe^{II}Cu^{II}$ compound **4** is 1.22 Nβ, which is significantly smaller than that (2.0 Nβ) of $S_T = 1$ spin ground state. However, such a decrease in M values takes place due to single-ion zero-field effect (*vide infra*; $D_{Fe} = 3.45\ cm^{-1}$).

The $Cu^{II}\cdots Cu^{II}$ distance in the $Cu^{II}Zn^{II}Cu^{II}$ compound **6** is 4.00 Å, indicating that the two copper(II) centres can interact through space or through the bis(μ-phenoxo)$\cdots Zn^{II}\cdots$bis(μ-phenoxo) long route and this is the only exchange interaction possible in **6**. Thus the HDvV spin Hamiltonian for this case is $H = -2JS_1S_3$ (where $S_1 = S_3 = 1/2$; Scheme 2). The main exchange interactions in **1–5** should be the two $Cu^{II}\cdots M^{II}$

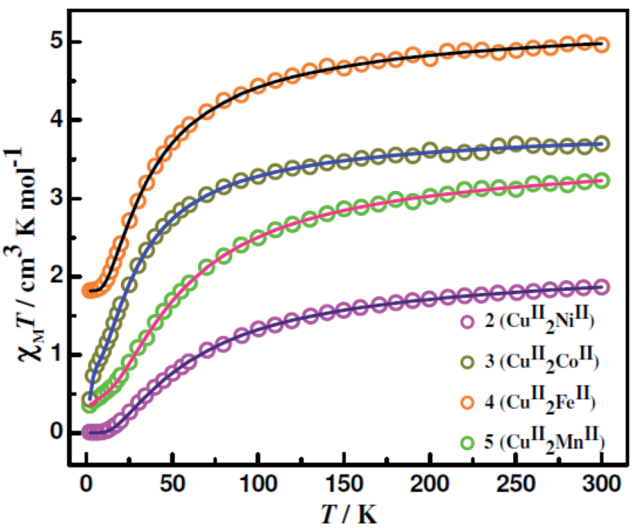

Fig. 8 Fitting of $\chi_M T$ *versus* T of **2–5** between 2 and 300 K. The experimental data are shown in symbols and the lines correspond to the fitted values.

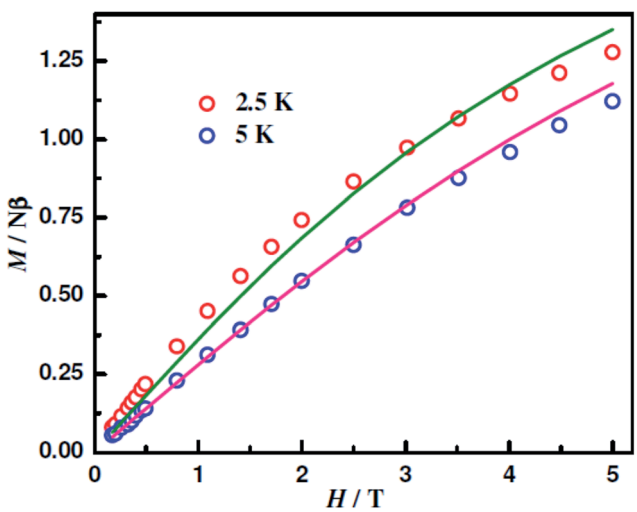

Fig. 10 Magnetization of $[\{Cu^{II}L(ClO_4)\}_2Fe^{II}(CH_3OH)_2]$ (**4**) at the indicated temperatures. The symbols are the experimental data, while the solid lines represent the fitted curves.

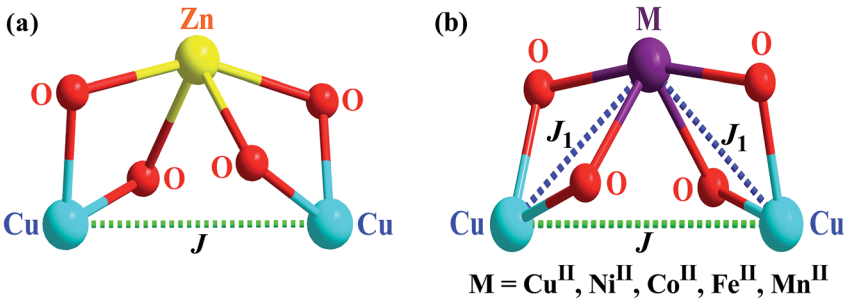

Scheme 2 Model of Magnetic exchange in **6** (a) and **1–5** (b).

interactions (M = Cu, Ni, Co, Fe, Mn) propagated *via* bis(μ-phenoxo) bridging moiety. In **1–5**, the Cu^{II} (in N_2O_2 site)$\cdots Cu^{II}$ (in N_2O_2 site) interaction should also be taken into account as the $Cu^{II}\cdots Cu^{II}$ distance lie in the range 4.09–5.80 Å (less than 6 Å). The two $Cu^{II}\cdots M^{II}$ interactions in **4** and **5** are the same as the two pairs are symmetry related. In each of **1–3**, the comparison of the values of the parameters in the two $Cu^{II}\cdots M^{II}$ pairs that can govern the magnetic exchange are as follows: (i) $Cu^{II}\cdots M^{II}$ distances are close (*vide supra*, Scheme S1†); (ii) the phenoxo bridge angles in the two pairs are not very different (average in two pairs: 99.05 and 96.85° in **1**, 96.99 and 95.62° in **2**, 97.06 and 96.89° in **3**; Table 3); (iii) Cu–O–M–O torsion angles (τ) are not very different (Table 3); (iv) Out-of-plane shift of the phenyl rings are not very different (Table 3). Hence, it is logical to assume the two $Cu^{II}\cdots M^{II}$ interactions as the same. Single-ion zero-field parameter should be considered for Ni^{II}, Co^{II} and Fe^{II}. So, the spin Hamiltonian for **1** ($Cu^{II}Cu^{II}Cu^{II}$) and **5** ($Cu^{II}Mn^{II}Cu^{II}$) is given by $H = -2J_1(S_1S_2 + S_3S_2) - 2JS_1S_3$ (where $S_1 = S_3 = 1/2$ and S_2 is 1/2 for **1** and 5/2 for **5**; Scheme 2) and for **2** ($Cu^{II}Ni^{II}Cu^{II}$), **3** ($Cu^{II}Co^{II}Cu^{II}$) and **4** ($Cu^{II}Fe^{II}Cu^{II}$) is given by eqn (1) (where $S_1 = S_3 = 1/2$ and S_2 is 1, 3/2 and 2, respectively; Scheme 2).

$$H = -2J_1(S_1S_2 + S_3S_2) - 2JS_1S_3 + D\left[S_{Z,2}{}^2 - \frac{1}{3}(S_2(S_2+1))\right] \quad (1)$$

Taking into consideration of the above mentioned models and also temperature independent paramagnetism (TIP) and different *g* values for different metal ions, the magnetic data of **1–6** were simulated with PHI software,[26] resulting in excellent fits with the following sets of converging parameters: $J_1 = -136.50\ cm^{-1}$, $J = 0.00$, $g = 2.09$ and TIP = $230 \times 10^{-6}\ cm^3\ mol^{-1}$ for the $Cu^{II}Cu^{II}Cu^{II}$ compound **1**; $J_1 = -22.16\ cm^{-1}$, $J = -1.97\ cm^{-1}$, $g_{Cu} = 2.10$, $g_{Ni} = 2.19$, $D_{Ni} = 1.64\ cm^{-1}$ and TIP = $315 \times 10^{-6}\ cm^3\ mol^{-1}$ for the $Cu^{II}Ni^{II}Cu^{II}$ compound **2**; $J_1 = -14.78\ cm^{-1}$, $J = -1.86\ cm^{-1}$, $g_{Cu} = 2.11$, $g_{Co} = 2.39$, $D_{Co} = 23.96\ cm^{-1}$ and TIP = $213 \times 10^{-6}\ cm^3\ mol^{-1}$ for the $Cu^{II}Co^{II}Cu^{II}$ compound **3**; $J_1 = -6.35\ cm^{-1}$, $J = -1.17\ cm^{-1}$, $g_{Cu} = 2.09$, $g_{Fe} = 2.01$, $D_{Fe} = 3.45\ cm^{-1}$ and TIP = $150 \times 10^{-6}\ cm^3\ mol^{-1}$ for the $Cu^{II}Fe^{II}Cu^{II}$ compound **4**; $J_1 = -6.02\ cm^{-1}$, $J = -1.70\ cm^{-1}$, $g_{Cu} = 2.07$, $g_{Mn} = 2.00$ and TIP = $212 \times 10^{-6}\ cm^3\ mol^{-1}$ for the $Cu^{II}Mn^{II}Cu^{II}$ compound **5**; $J = -2.25\ cm^{-1}$, $g = 2.12$ and TIP = $165 \times 10^{-6}\ cm^3\ mol^{-1}$ for the $Cu^{II}Zn^{II}Cu^{II}$ compound **6**. Notably, both $\chi_M T$ *versus* *T* and *M* *versus* *H* data of **1**, **3**, **4** and **5** were simulated contemporaneously.

The order of the extent of antiferromagnetic interactions through bis(μ-phenoxo) route in **1–5** are as follows: $Cu^{II}Cu^{II}Cu^{II}$ (**1**; $J_1 = -136.50\ cm^{-1}$) > $Cu^{II}Ni^{II}Cu^{II}$ (**2**; $J_1 = -22.16\ cm^{-1}$) > $Cu^{II}Co^{II}Cu^{II}$ (**3**; $J_1 = -14.78\ cm^{-1}$) > $Cu^{II}Fe^{II}Cu^{II}$ (**4**; $J_1 = -6.35\ cm^{-1}$) ≈ $Cu^{II}Mn^{II}Cu^{II}$ (**5**; $J_1 = -6.02\ cm^{-1}$). As the geometry of the copper(II) centre in the $O(phenoxo)_4$ site of the two ligands in **1** is intermediate between square pyramidal and trigonal bipyramidal and that of other metal ions in the similar site in **2–4** is distorted octahedral, it is complicated to explain the overall trend in terms of orbital model without theoretical calculations. However, assuming $d_{x^2-y^2}$ as the magnetic orbital of all the copper(II) centres in **1–5**, the trend can be qualitatively explained on the basis of magnetic orbitals.[1a,11b,27] While the magnetic orbital for copper(II) is only one ($d_{x^2-y^2}$), the number of magnetic orbitals increases on going from copper(II) to manganese(II). Of the different types of orbital combinations, only $d_{x^2-y^2} \leftrightarrow d_{x^2-y^2}$ is antiferromagnetic, whereas other combinations are ferromagnetic. As a result, the order of ferromagnetic contributions in the five compounds **1–5** should be $Cu^{II}Mn^{II}Cu^{II}$ > $Cu^{II}Fe^{II}Cu^{II}$ > $Cu^{II}Co^{II}Cu^{II}$ > $Cu^{II}Ni^{II}Cu^{II}$ > $Cu^{II}Cu^{II}Cu^{II}$. Therefore, the order of the extent of antiferromagnetic interaction should be $Cu^{II}Cu^{II}Cu^{II}$ > $Cu^{II}Ni^{II}Cu^{II}$ > $Cu^{II}Co^{II}Cu^{II}$ > $Cu^{II}Fe^{II}Cu^{II}$ > $Cu^{II}Mn^{II}Cu^{II}$, which is almost matched with the observed trend.

Previously, a number of magneto-structural correlations were established in bis(μ-hydroxo/alkoxo/phenoxo) dicopper(II) compounds.[3,4a–c,5] Based on experimental magnetic properties in planar dihydroxo-bridged dicopper(II) systems, it was established that the magnetic exchange interaction should be ferromagnetic and antiferromagnetic, respectively, if the Cu–O–Cu bridge angle (α) is, respectively, smaller than and greater than a cross-over angle of around 97.5°.[3] Later, based on density functional theoretical calculations in dihydroxo/dialkoxo/diphenoxo-bridged dicopper(II) systems, it has been established that the out-of-plane shift (φ) of the hydrogen atom/alkyl group/phenyl group is also a major factor and the hinge distortion (τ) of the Cu_2O_2 plane has also some role to govern the interaction.[4a–c] Some salient features of the DFT calculations may be summarized as follows: (i) if $\varphi = 35°$ and $\tau = 20°$ in bis(μ-hydroxo) dicopper(II) systems and $\varphi = 50°$ in

bis(μ-phenoxo) dicopper(II) systems, the interaction is ferromagnetic and α has practically no role to switch the interaction to antiferromagnetic; (ii) if $\varphi = 0°$ and $\tau = 0°$ in bis(μ-hydroxo) dicopper(II) systems and $\varphi = 0°$ in bis(μ-phenoxo) dicopper(II) systems, J changes linearly with α where the more the α the more the antiferromagnetic interaction but the cross-over takes place at around 90° and 83° for the hydroxo and phenoxo systems, respectively. Hence, although larger α and smaller φ and τ favour antiferromagnetic interaction and *vice versa*, it is problematic to get a magneto-structural correlation based on experimental J values in compounds derived from different types of ligands as variation of one parameter on keeping two of the three parameters more or less similar is difficult. Moreover, the theoretical correlations were done on planar Cu_2O_2 complexes, where both copper(II) ions are square planar, which makes it more difficult to absolutely correlate the experimental J values with the theoretical correlations. However, the theoretical correlations are nice enough to qualitatively rationalize the magnetic exchange interactions of new systems. It is also worth mentioning that correlations established in diphenoxo-bridged dicopper(II) systems should be more or less similar in trinuclear Cu^{II}–bis(μ-phenoxo)–Cu^{II}–bis(μ-phenoxo)–Cu^{II} systems like **1**. In **1**, although the coordination environment of two Cu^{II} centres is distorted, that of one copper(II) centre (Cu3) is intermediate between square pyramidal and trigonal bipyramidal and hence this system is quite different from the models utilized in establishing theoretical correlations. However, average values of α (97.95°), φ (7.02°) and τ (15.35°) indicate that the interaction in **1** should not be ferromagnetic or strong antiferromagnetic, which is actually observed; the interaction is moderately strong in **1** with $J = -136.5$ cm^{-1}. The J, α, φ and τ values of the structurally and magnetically characterized Cu^{II}–bis(μ-phenoxo)–Cu^{II}–bis(μ-phenoxo)–Cu^{II} systems[5,14g,17c,20c,27b,28] are compared in Table S5† and J *versus* α, J *versus* φ and J *versus* τ plots are shown in Fig. S14–S16,† respectively, revealing that there is no correlation in experimental magnetic properties due to the reason already explained.

Till date, no magneto-structural correlation in $Cu^{II}M^{II}$ compounds (M = Ni, Co, Fe, Mn) has been reported. However, it can be anticipated that above mentioned three parameters α, φ and τ should have roles in governing the nature and magnitude of magnetic exchange interaction in diphenoxo-bridged systems, such as in the $Cu^{II}M^{II}Cu^{II}$ compounds **2–5**. In all these four compounds, the out-of-plane shift of the phenyl group is small (average $\varphi = 6.92–8.55°$), favouring strong antiferromagnetic interaction. However, the hinge angle values are sufficiently large (average $\tau = 20.44–23.25°$) and the phenoxo bridge angle values are sufficiently smaller (average $\alpha = 96.31–97.05°$) to reduce the antiferromagnetic interaction. In balance, the magnetic exchange interaction is **2–5** is weak or moderate antiferromagnetic with J (Cu^{II}–M^{II}) values of −22.16, −14.78, −6.35 and −6.02 cm^{-1}, respectively.

The J, α, φ and τ values of the known compounds having diphenoxo bridged $Cu^{II}M^{II}$ species are listed in Tables S6† (for $Cu^{II}Ni^{II}$),[13a,15a,29] Tables S7† (for $Cu^{II}Co^{II}$),[13g,16a,17a,b,g,19h,20e,23a,29d,30] Table 5 (for $Cu^{II}Fe^{II}$)[17b,20a,23b] and Tables S8† (for $Cu^{II}Mn^{II}$).[13d,15a,17a,f,19h,m,20a,b,d,23a,e,29e,31] The nature of interaction in Cu^{II}–bis(μ-phenoxo)–M^{II} moieties in all but one previously reported compounds is antiferromagnetic with J values lying in the ranges from −3.53 to −130.0, from −7.3 to −53.3, from −6 to −36.9 and from −6.35 to −36.8 cm^{-1}, respectively, for the Ni^{II}, Co^{II}, Fe^{II} and Mn^{II} analogues; the sole system exhibiting ferromagnetic interaction is a $Mn^{II}Cu^{II}_3$ star with J value of 1.02 cm^{-1}. Hence the J (Cu^{II}–M^{II}) values of −22.16, −14.78,

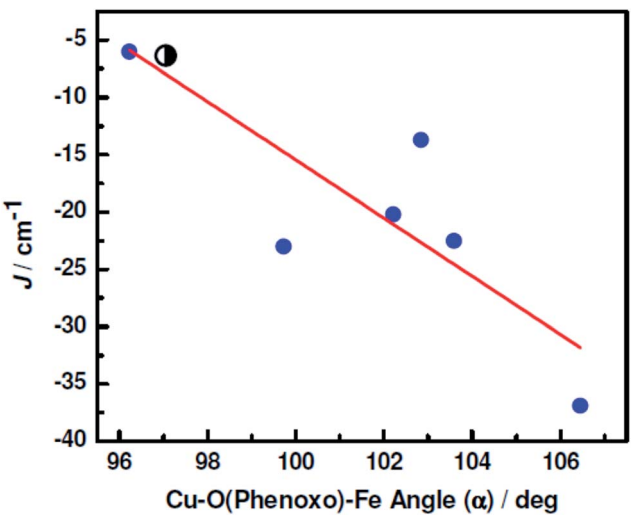

Fig. 11 *J versus* Cu–O(phenoxo)–Fe bridge angle magneto-structural correlation in diphenoxo-bridged $Cu^{II}Fe^{II}$ compounds. Blue filled circles: data of previous compounds. Black-white half-filled circle: data of compound **4**.

Table 5 Magnetic exchange integral and some relevant structural parameters of the systems where copper(II) and iron(II) centres are bridged by solely bis(μ_2-phenoxo) moiety

Compound no.	CSD code	J (cm^{-1})	Average Cu–O(phenoxo)–Fe bridge angle (α) (in °)	Out-of-plane shift of phenyl group (φ) (in °)	Cu–O–Fe–O torsion angle (τ) (in °)	Reference
1	BICBEW	−20.2	102.21	6.57	8.40	20*a*
2	BICBOG	−36.9	106.45	2.91	5.45	20*a*
3	FIHFAD	−6	96.23	11.72	26.54	17*b*
4	FIHFEH	−23	99.72	24.55	27.56	17*b*
5	IVOVOF	−22.5	103.58	6.51	1.70	23*b*
6	IVOVUL	−13.7	102.84	6.27	3.83	23*b*
7	—	−6.35	97.01	7.58	23.23	This work

−6.35 and −6.02 cm^{-1} in **2–5**, respectively, lie well in the ranges of the known compounds. However, the *J versus* $\alpha/\varphi/\tau$ plots for the Ni^{II} (Fig. S17–S19†), Co^{II} (Fig. S20–S22†) and Mn^{II} (Fig. S23–S25†) analogues show that it is not possible to establish a magneto-structural correlation; the graphs are significantly scattered. The same is the case for the *J versus* φ/τ plots (Fig. S26 and S27†) for the systems having diphenoxo bridged $Cu^{II}Fe^{II}$ species. On the other hand, a linear correlation (Fig. 11) can be established between the *J* and α values in diphenoxo bridged $Cu^{II}Fe^{II}$ compound and that is $J = -2.54\alpha + 238.61$. According to this correlation the cross-over angle in diphenoxo-bridged $Cu^{II}Fe^{II}$ systems is 93.9°. However, the correlation should not be considered as strong as the number of data points is small in comparison to those in other $Cu^{II}M^{II}$ systems (M = Ni, Co, Mn).

Conclusions

Six $Cu^{II}M^{II}Cu^{II}$ compounds, **1** (M = Cu), **2** (M = Ni), **3** (M = Co), **4** (M = Fe), **5** (M = Mn) and **6** (M = Zn), are only the third examples of copper(II)–second metal ion systems, next to the previously reported a $Cu^{II}Hg^{II}$ and a $Cu^{II}{}_2Gd^{III}{}_2$ compound,[24] derived from salicylaldehyde-*trans*-1,2-diaminocyclohexane ligand, H_2L. This aspect deserves attention as many copper(II)–second metal ion compounds are known from a number of closely similar ligands. The complications in isolating most of the compounds of **1–6** in crystalline form may be taken as a reason why this particular ligand has been remained so little explored to derive/report copper(II)–second metal ion systems. This is the second ligand system among salicylaldehyde/2-hydroxyacetophenone/2-hydroxypropiophenone/3-methoxysalicylaldehyde/3-ethoxysalicylaldehyde–diamine ligands in which all the six copper(II)–second metal ion compounds with Mn^{II}–Zn^{II} as the second metal ions are reported. However, in comparison to the sole earlier case,[23a–d] all the six compounds herein have basically similar composition (trinuclear $Cu^{II}M^{II}Cu^{II}$).

ESI-MS positive of **1–6** reveal some interesting features. For example, stabilization of heterometallic star ions for all the five heterometallic trinuclear compounds **2–6** may be mentioned. Again, although the most intense signal in all the six ESI-MS correspond to trinuclear ions, the nature is of two types; $Cu^{II}M^{II}Cu^{II}$ for the Cu^{II}, Ni^{II}, Co^{II}, Fe^{II} and Zn^{II} analogues but $Cu^{II}Mn^{I}Cu^{II}$ for the Mn^{II} analogue **5**.

One or more O–H···O/C–H···O hydrogen bond (s) exist (s) in **1–6**. The trinuclear units in **1**, **3** and **4–6** are interlinked by hydrogen bonds to generate following types of supramolecular self-assemblies: dimeric in **1**, one-dimensional in **3** and three-dimensional in **4–6**.

Variable-temperature and variable-field magnetic studies reveal moderate or weak antiferromagnetic interaction between Cu^{II} and M^{II} (M = Cu, Ni, Co, Fe, Mn) through diphenoxo bridge and very weak antiferromagnetic interaction between the two Cu^{II} in the $N(imine)_2O(phenoxo)_2$ compartments in **1–6**. We have compared the magnetic exchange integrals and the key structural parameters of the previously reported homo/heterometallic systems having diphenoxo bridging moiety between the two metal ions. However, no correlation exists for the other systems except $Cu^{II}Fe^{II}$. In the case of the latter, a linear correlation between *J* and Cu^{II}–O(phenoxo)–Fe^{II} bridge angle is established, although the relationship should not be considered as a strong one as the number of data points is rather limited in comparison to those of other systems.

We hope this particular ligand H_2L henceforth will draw the attention of the coordination chemistry community, having particular interest in stabilizing heterometallic systems from salicylaldehyde/2-hydroxyacetophenone/2-hydroxypropiophenone/3-methoxysalicylaldehyde/3-ethoxysalicylaldehyde–diamine Schiff base ligands.

Conflicts of interest

There are no conflicts of interest to declare.

Acknowledgements

Financial support for this work has been received from Government of India through University Grants Commission (contingency from CAS-V project to S. Mohanta; Women Post-doctoral Fellowship to A. Jana; JRF/SRF to N. Hari) and Department of Science and Technology (INSPIRE Fellowship to Shuvankar Mandal). Crystallography and ESI-MS were performed at the DST-FIST-funded Single Crystal Diffractometer Facility and DST-PURSE-funded Mass Spectrometer facility, both at the Department of Chemistry, University of Calcutta. Centre for Research in Nanoscience and Nanotechnology, University of Calcutta, is acknowledged for magnetic data.

References

1 (*a*) O. Kahn, *Molecular Magnetism*, VCH Publications, New York, 1993; (*b*) *Magneto-Structural Correlations in Exchange Coupled Systems*, ed. R. D. Willet, D. Gatteschi and O. Kahn, Reidel, Dordrecht, The Netherlands, 1985.

2 (*a*) B. C. Guha, *Proc. Roy. Soc. Lond.*, 1951, **A206**, 353; (*b*) B. Bleaney and K. D. Bowers, *Proc. Roy. Soc. Lond.*, 1952, **A214**, 451.

3 V. H. Crawford, H. W. Richardson, J. R. Wasson, D. J. Hodgson and W. E. Hatfield, *Inorg. Chem.*, 1976, **15**, 2107.

4 (*a*) D. Venegas-Yazigi, D. Aravena, E. Spodine, E. Ruiz and S. Alvarez, *Coord. Chem. Rev.*, 2010, **254**, 2086; (*b*) E. Ruiz, P. Alemany, S. Alvarez and J. Cano, *Inorg. Chem.*, 1997, **36**, 3683; (*c*) E. Ruiz, C. de Graaf, P. Alemany and S. Alvarez, *J. Phys. Chem. A*, 2002, **106**, 4938; (*d*) A. Rodríguez-Fortea, P. Alemany, S. Alvarez and E. Ruiz, *Inorg. Chem.*, 2002, **41**, 3769; (*e*) E. Ruiz, J. Cano, S. Alvarez and P. Alemany, *J. Am. Chem. Soc.*, 1998, **120**, 11122; (*f*) S. Triki, C. J. Gómez-García, E. Ruiz and J. Sala-Pala, *Inorg. Chem.*, 2005, **44**, 5501; (*g*) F. F. de Biani, E. Ruiz, J. Cano, J. J. Novoa and S. Alvarez, *Inorg. Chem.*, 2000, **39**, 3221.

5 L. Botana, J. Ruiz, J. M. Seco, A. J. Mota, A. Rodríguez-Diéguez, R. Sillanpää and E. Colacio, *Dalton Trans.*, 2011, **40**, 12462.

6 L. Merz and W. Haase, *J. Chem. Soc., Dalton Trans.*, 1980, 875.

7 (*a*) K. K. Nanda, L. K. Thompson, J. N. Bridson and K. Nag, *Chem. Commun.*, 1994, 1337; (*b*) M. A. Palacios, A. J. Mota, J. E. Perea-Buceta, F. J. White, E. K. Brechin and E. Colacio, *Inorg. Chem.*, 2010, **49**, 10156; (*c*) S. Sasmal, S. Hazra, P. Kundu, S. Dutta, G. Rajaraman, E. C. Sañudo and S. Mohanta, *Inorg. Chem.*, 2011, **50**, 7257.

8 S. Sasmal, S. Hazra, P. Kundu, S. Majumder, N. Aliaga-Alcalde, E. Ruiz and S. Mohanta, *Inorg. Chem.*, 2010, **49**, 9517.

9 (*a*) D. M. Kurtz Jr, *Chem. Rev.*, 1990, **90**, 585; (*b*) F. L. Gall, F. F. de Biani, A. Caneschi, P. Cinelli, A. Cornia, A. C. Fabretti and D. Gatteschi, *Inorg. Chim. Acta*, 1997, **262**, 123; (*c*) C. Cañada-Vilalta, T. A. O'Brien, E. K. Brechin, M. Pink, E. R. Davidson and G. Christou, *Inorg. Chem.*, 2004, **43**, 5505; (*d*) N. Berg, T. Rajeshkumar, S. M. Taylor, E. K. Brechin, G. Rajaraman and L. F. Jones, *Chem.–Eur. J.*, 2012, **18**, 5906; (*e*) A. Niemann, U. Bossek, K. Wieghardt, C. Butzlaff, A. X. Trautwein and B. Nuber, *Angew. Chem., Int. Ed. Engl.*, 1992, **31**, 311.

10 T. Rajeshkumar and G. Rajaraman, *Chem. Commun.*, 2012, **48**, 7856.

11 (*a*) J.-P. Costes, F. Dahan and A. Dupuis, *Inorg. Chem.*, 2000, **39**, 165; (*b*) S. Mohanta, K. K. Nanda, L. K. Thompson, U. Flörke and K. Nag, *Inorg. Chem.*, 1998, **37**, 1465; (*c*) S. Sasmal, S. Roy, L. Carrella, A. Jana, E. Rentschler and S. Mohanta, *Eur. J. Inorg. Chem.*, 2015, 680; (*d*) G. Rajaraman, F. Totti, A. Bencini, A. Caneschi, R. Sessoli and D. Gatteschi, *Dalton Trans.*, 2009, 3153; (*e*) S. K. Singh, N. K. Tibrewal and G. Rajaraman, *Dalton Trans.*, 2011, **40**, 10897; (*f*) S. Hazra, S. Bhattacharya, M. K. Singh, L. Carrella, E. Rentschler, T. Weyhermueller, G. Rajaraman and S. Mohanta, *Inorg. Chem.*, 2013, **52**, 12881.

12 *The Cambridge Structural Database (CSD), version 5.37*, The Cambridge Crystallographic Data Centre (CCDC), 2016.

13 (*a*) Y. Journaux, O. Kahn, I. Morgenstern-Badarau, J. Galy, J. Jaud, A. Bencini and D. Gatteschi, *J. Am. Chem. Soc.*, 1985, **107**, 6305; (*b*) A. Bencini, C. Benelli, A. Caneschi, R. L. Carlin, A. Dei and D. Gatteschi, *J. Am. Chem. Soc.*, 1985, **107**, 8128; (*c*) G. A. Brewer and E. Sinn, *Inorg. Chim. Acta*, 1987, **134**, 13; (*d*) R. Ruiz, F. Lloret, M. Julve and J. Faus, *Inorg. Chim. Acta*, 1993, **213**, 261; (*e*) I. Ramade, O. Kahn, Y. Jeannin and F. Robert, *Inorg. Chem.*, 1997, **36**, 930; (*f*) M. Ryazanov, V. Nikiforov, F. Lloret, M. Julve, N. Kuzmina and A. Gleizes, *Inorg. Chem.*, 2002, **41**, 1816; (*g*) A. Gutiérrez, M. F. Perpiñán, A. E. Sánchez, M. C. Torralba and M. R. Torres, *Inorg. Chim. Acta*, 2010, **363**, 1837; (*h*) F. Pointillart and K. Bernot, *Eur. J. Inorg. Chem.*, 2010, 952; (*i*) A. Biswas, S. Mondal, L. Mandal, A. Jana, P. Chakraborty and S. Mohanta, *Inorg. Chim. Acta*, 2014, **414**, 199.

14 (*a*) D. W. Harrison and J.-C. G. Bdnzli, *Inorg. Chim. Acta*, 1985, **109**, 185; (*b*) G. Novitchi, S. Shova, A. Caneschi, J.-P. Costes, M. Gdaniec and N. Stanica, *Dalton Trans.*, 2004, 1194; (*c*) Q. Shi, L. Sheng, K. Ma, Y. Sun, X. Cai, R. Liu and S. Wang, *Inorg. Chem. Commun.*, 2009, **12**, 255; (*d*) I. Gamba, P. Gamez, E. Monzani, L. Casella, I. Mutikainen and J. Reedijk, *Eur. J. Inorg. Chem.*, 2011, 4360; (*e*) Z.-L. You, Y. Lu, N. Zhang, B.-W. Ding, H. Sun, P. Hou and C. Wang, *Polyhedron*, 2011, **30**, 2186; (*f*) R. Vafazadeh, B. Khaledi, A. C. Willis and M. Namazian, *Polyhedron*, 2011, **30**, 1815; (*g*) S. Saha, A. Sasmal, C. Roy Choudhury, C. J. Gómez-Garcia, E. Garribba and S. Mitra, *Polyhedron*, 2014, **69**, 262; (*h*) L. Mandal, S. Bhattacharya and S. Mohanta, *Inorg. Chim. Acta*, 2013, **406**, 87; (*i*) P. Chakraborty and S. Mohanta, *Inorg. Chim. Acta*, 2017, **455**, 70.

15 (*a*) S. Mondal, S. Mandal, L. Carrella, A. Jana, M. Fleck, A. Köhn, E. Rentschler and S. Mohanta, *Inorg. Chem.*, 2015, **54**, 117; (*b*) S. Mondal, S. Mandal, A. Jana and S. Mohanta, *Inorg. Chim. Acta*, 2014, **415**, 138; (*c*) L. T. Yildirim, R. Kurtaran, H. Namli, A. D. Azaz and O. Atakol, *Polyhedron*, 2007, **26**, 4187.

16 (*a*) R.-J. Tao, F.-A. Li, S.-Q. Zang, Y.-X. Cheng, Q.-L. Wang, J.-Y. Niu and D.-Z. Liao, *J. Coord. Chem.*, 2006, **59**, 901; (*b*) S. Bandyopadhyay, J.-M. Lo, H.-H. Yao, F.-L. Liao and P. Chattopadhyay, *J. Coord. Chem.*, 2006, **59**, 2015; (*c*) A. Bhunia, P. W. Roesky, Y. Lan, G. E. Kostakis and A. K. Powell, *Inorg. Chem.*, 2009, **48**, 10483.

17 (*a*) C. J. O'connor, D. P. Freyberg and E. Sinn, *Inorg. Chem.*, 1979, **18**, 1077; (*b*) G. A. Brewer and E. Sinn, *Inorg. Chem.*, 1987, **26**, 1529; (*c*) P. Talukder, S. Shit, A. Sasmal, S. R. Batten, B. Moubaraki, K. S. Murray and S. Mitra, *Polyhedron*, 2011, **30**, 1767; (*d*) I. Morgenstern-Badarau, D. Laroque, E. Bill, H. Winkler, A. X. Trautwein, F. Robert and Y. Jeannin, *Inorg. Chem.*, 1991, **30**, 3180; (*e*) C. Brewer, G. Brewer, W. R. Scheidt, M. Shang and E. E. Carpenter, *Inorg. Chim. Acta*, 2001, **313**, 65; (*f*) S. Biswas, S. Naiya, C. J. Gomez-Garcia and A. Ghosh, *Dalton Trans.*, 2012, **41**, 462; (*g*) S. Biswas, C. J. Gómez-García, J. M. Clemente-Juan, S. Benmansour and A. Ghosh, *Inorg. Chem.*, 2014, **53**, 2441.

18 M. Andruh, D. G. Branzea, R. Gheorghe and A. M. Madalan, *CrystEngComm*, 2009, **11**, 2555.

19 (*a*) J.-P. Costes, F. Dahan, A. Dupuis and J.-P. Laurent, *Inorg. Chem.*, 1996, **35**, 2400; (*b*) J.-P. Costes, F. Dahan, A. Dupuis and J.-P. Laurent, *Chem.–Eur. J.*, 1998, **4**, 1616; (*c*) O. Margeat, P. G. Lacroix, J. P. Costes, B. Donnadieu and C. Lepetit, *Inorg. Chem.*, 2004, **43**, 4743; (*d*) J.-P. Costes, B. Donnadieu, R. Gheorghe, G. Novitchi, J.-P. Tuchagues and L. Vendier, *Eur. J. Inorg. Chem.*, 2008, 5235; (*e*) D. Visinescu, I.-R. Jeon, A. M. Madalan, M.-G. Alexandru, B. Jurca, C. Mathoniere, R. Clerac and M. Andruh, *Dalton Trans.*, 2012, **41**, 13578; (*f*) N. Bridonneau, L.-M. Chamoreau, P. P. Lainé, W. Wernsdorferc and V. Marvaud, *Chem. Commun.*, 2013, **49**, 9476; (*g*) J. Long, L.-M. Chamoreau and V. Marvaud, *Dalton Trans.*, 2010, **39**, 2188; (*h*) S. Osa, Y. Sunatsuki, Y. Yamamoto, M. Nakamura, T. Shimamoto, N. Matsumoto and N. Re, *Inorg. Chem.*, 2003, **42**, 5507; (*i*) S. Bhattacharya, A. Jana and S. Mohanta, *CrystEngComm*, 2013, **15**, 10374; (*j*) S. Majumder, R. Koner, P. Lemoine, M. Nayak, M. Ghosh, S. Hazra, C. R. Lucas and S. Mohanta, *Eur. J. Inorg. Chem.*, 2009, 3447; (*k*) A. Biswas, S. Mondal and S. Mohanta, *J. Coord. Chem.*, 2013, **66**, 152; (*l*) S. Bhattacharya, A. Jana and S. Mohanta, *Polyhedron*, 2013, **62**, 234; (*m*) A. Biswas,

M. Ghosh, P. Lemoine, S. Sarkar, S. Hazra and S. Mohanta, *Eur. J. Inorg. Chem.*, 2010, 3125.

20 (*a*) A. Biswas, L. Mandal, S. Mondal, C. R. Lucas and S. Mohanta, *CrystEngComm*, 2013, **15**, 5888; (*b*) D. G. Branzea, A. M. Madalan, S. Ciattini, N. Avarvari, A. Caneschi and M. Andruh, *New J. Chem.*, 2010, **34**, 2479; (*c*) S. Thakurta, C. Rizzoli, R. J. Butcher, C. J. Gómez-García, E. Garribba and S. Mitra, *Inorg. Chim. Acta*, 2010, **363**, 1395; (*d*) D. G. Branzea, A. Guerri, O. Fabelo, C. Ruiz-Pérez, L.-M. Chamoreau, C. Sangregorio, A. Caneschi and M. Andruh, *Cryst. Growth Des.*, 2008, **8**, 941; (*e*) J.-P. Costes, R. Gheorghe, M. Andruh, S. Shova and J.-M. C. Juan, *New J. Chem.*, 2006, **30**, 572.

21 (*a*) T. Kajiwara, M. Nakano, K. Takahashi, S. Takaishi and M. Yamashita, *Chem.–Eur. J.*, 2011, **17**, 196; (*b*) R. Gheorghe, P. Cucos, M. Andruh, J.-P. Costes, B. Donnadieu and S. Shova, *Chem.–Eur. J.*, 2006, **12**, 187; (*c*) X.-C. Huang, C. Zhou, H.-Y. Wei and X.-Y. Wang, *Inorg. Chem.*, 2013, **52**, 7314.

22 A. Jana and S. Mohanta, *CrystEngComm*, 2014, **16**, 5494.

23 (*a*) M. Nayak, R. Koner, H.-H. Lin, U. Flörke, H.-H. Wei and S. Mohanta, *Inorg. Chem.*, 2006, **45**, 10764; (*b*) A. Jana, R. Koner, T. Weyhermueller, P. Lemoine, M. Ghosh and S. Mohanta, *Inorg. Chim. Acta*, 2011, **375**, 263; (*c*) A. Jana, R. Koner, M. Nayak, P. Lemoine, S. Dutta, M. Ghosh and S. Mohanta, *Inorg. Chim. Acta*, 2011, **365**, 71; (*d*) M. Nayak, S. Sarkar, S. Hazra, H. A. Sparkes, J. A. K. Howard and S. Mohanta, *CrystEngComm*, 2011, **13**, 124; (*e*) M. Nayak, S. Hazra, P. Lemoine, R. Koner, C. R. Lucas and S. Mohanta, *Polyhedron*, 2008, **27**, 1201; (*f*) R. Koner, H.-H. Lin, H.-H. Wei and S. Mohanta, *Inorg. Chem.*, 2005, **44**, 3524; (*g*) A. Jana, S. Majumder, L. Carrella, M. Nayak, T. Weyhermüeller, S. Dutta, D. Schollmeyer, E. Rentschler, R. Koner and S. Mohanta, *Inorg. Chem.*, 2010, **49**, 9012; (*h*) M. Nayak, A. Jana, M. Fleck, S. Hazra and S. Mohanta, *CrystEngComm*, 2010, **12**, 1416; (*i*) S. Sasmal, S. Majumder, S. Hazra, H. A. Sparkes, J. A. K. Howard, M. Nayak and S. Mohanta, *CrystEngComm*, 2010, **12**, 4131.

24 (*a*) M. L. Colon, S. Y. Qian, D. Vanderveer and X. R. Bu, *Inorg. Chim. Acta*, 2004, **357**, 83; (*b*) J.-P. Costes, C. Duhayon, S. Mallet-Ladeira, S. Shova and L. Vendier, *Chem.–Eur. J.*, 2016, **22**, 2171.

25 (*a*) Bruker-Nonius, *APEX-II, SAINT-Plus and TWINABS*, Bruker-Nonius AXS Inc., Madison, Wisconsin, USA, 2004; (*b*) G. M. Sheldrick, *SAINT (Version 6.02), SADABS (Version 2.03)*, Bruker AXS lnc., Madison, Wisconsin, 2002; (*c*) G. M. Sheldrick, *Acta Crystallogr., Sect. A: Found. Crystallogr.*, 2008, **64**, 112; (*d*) G. M. Sheldrick, *Acta Crystallogr., Sect. C: Struct. Chem.*, 2015, **71**, 3; (*e*) A. L. Spek, *J. Appl. Crystallogr.*, 2003, **36**, 7; (*f*) A. L. Spek, *Acta Crystallogr., Sect. D: Biol. Crystallogr.*, 2009, **65**, 148.

26 N. F. Chilton, R. P. Anderson, L. D. Turner, A. Soncini and K. S. Murray, *J. Comput. Chem.*, 2013, **34**, 1164.

27 (*a*) F. Birkelbach, M. Winter, U. Flörke, H.-J. Haupt, C. Butzlaff, M. Lengen, E. Bill, A. X. Trautwein, K. Wieghardt and P. Chaudhuri, *Inorg. Chem.*, 1994, **33**, 3990; (*b*) M. Yonemura, K. Arimura, K. Inoue, N. Usuki, M. Ohba and H. Ohkawa, *Inorg. Chem.*, 2002, **41**, 582.

28 (*a*) Y.-F. Song, G. A. van Albada, J. Tang, I. Mutikainen, U. Turpeinen, C. Massera, O. Roubeau, J. S. Costa, P. Gamez and J. Reedijk, *Inorg. Chem.*, 2007, **46**, 4944; (*b*) X.-H. Bu, M. Du, Z.-L. Shang, R.-H. Zhang, D.-Z. Liao, M. Shionoya and T. Clifford, *Inorg. Chem.*, 2000, **39**, 4190; (*c*) Y. Song, P. Gamez, O. Roubeau, I. Mutikainen, U. Turpeinen and J. Reedijk, *Inorg. Chim. Acta*, 2005, **358**, 109; (*d*) M. Du, X.-J. Zhao, J.-H. Guo, X.-H. Bu and J. Ribas, *Eur. J. Inorg. Chem.*, 2005, 294; (*e*) Y. F. Song, G. A. van Albada, M. Quesada, I. Mutikainen, U. Turpeinen and J. Reedijk, *Inorg. Chem. Commun.*, 2005, **8**, 975; (*f*) Y. Song, P. Gamez, O. Roubeau, M. Lutz, A. L. Spek and J. Reedijk, *Eur. J. Inorg. Chem.*, 2003, 2924.

29 (*a*) C. N. Verani, E. Rentschler, T. Weyhermüller, E. Bill and P. Chaudhuri, *Dalton Trans.*, 2000, 251; (*b*) C. N. Verani, T. Weyhermüller, E. Rentschler, E. Bill and P. Chaudhuri, *Chem. Commun.*, 1998, 2475; (*c*) M. Yonemura, M. Ohba, K. Takahashi, H. Ōkawa and D. E. Fenton, *Inorg. Chim. Acta*, 1998, **283**, 72; (*d*) R.-J. Tao, C.-Z. Mei, S.-Q. Zang, Q.-L. Wang, J.-Y. Niu and D.-Z. Liao, *Inorg. Chim. Acta*, 2004, **357**, 1985; (*e*) A. Hori, Y. Mitsuka, M. Ohba and H. Ōkawa, *Inorg. Chim. Acta*, 2002, **337**, 113; (*f*) T. Aono, H. Wada, Y.-I. Aratake, N. Matsumoto, H. Ōkawa and Y. Matsuda, *J. Chem. Soc., Dalton Trans.*, 1996, 25; (*g*) I. Morgenstern-Badarau, M. Rerat, O. Khan, J. Jaud and J. Galy, *Inorg. Chem.*, 1982, **21**, 3050.

30 (*a*) R.-J. Tao, F.-A. Li, S.-Q. Zang, Y.-X. Cheng, Q.-L. Wang, J.-Y. Niu and D.-Z. Liao, *Polyhedron*, 2006, **25**, 2153; (*b*) Y. Sunatsuki, T. Matsuo, M. Nakamura, F. Kai, N. Matsumoto and J.-P. Tuchagues, *Bull. Chem. Soc. Jpn.*, 1998, **71**, 2611; (*c*) S. Ghosh, G. Aromí, P. Gamez and A. Ghosh, *Eur. J. Inorg. Chem.*, 2014, 3341.

31 (*a*) L. Bo, Z. Hong, P. Zhi-Quan, S. You, W. Cheng-Gang, Z. Han-Ping, H. Jing-Dong and C. Ru-An, *J. Coord. Chem.*, 2006, **59**, 1271; (*b*) D. Visinescu, J.-P. Sutter, C. Ruiz-Pérez and M. Andruh, *Inorg. Chim. Acta*, 2006, **359**, 433; (*c*) M. Pascu, F. Lloret, N. Avarvari, M. Julve and M. Andruh, *Inorg. Chem.*, 2004, **43**, 5189; (*d*) H. Ōkawa, J. Nishio, M. Ohba, M. Tadokoro, N. Matsumoto, M. Koikawa, S. Kida and D. E. Fenton, *Inorg. Chem.*, 1993, **32**, 2949.